Remote Sensing of Environment 190 (2017) 42–55

Contents lists available at ScienceDirect

Remote Sensing of Environment

journal homepage: www.elsevier.com/locate/rse

Modeling gross primary production of paddy rice cropland through analyses of data from CO_2 eddy flux tower sites and MODIS images

Fengfei Xin [a], Xiangming Xiao [a,b,*], Bin Zhao [a], Akira Miyata [c], Dennis Baldocchi [d], Sara Knox [d], Minseok Kang [e], Kyo-moon Shim [f], Sunghyun Min [f], Bangqian Chen [a,g], Xiangping Li [a], Jie Wang [b], Jinwei Dong [b,h], Chandrashekhar Biradar [i]

[a] Ministry of Education Key Laboratory of Biodiversity Science and Ecological Engineering, Institute of Biodiversity Science, Fudan University, Shanghai 200433, China
[b] Department of Microbiology and Plant Biology, Center for Spatial Analysis, University of Oklahoma, Norman, OK 73019, USA
[c] Division of Climate Change, Institute for Agro-Environmental Sciences, NARO, Tsukuba, 305-8604, Japan
[d] Department of Environmental Science, Policy and management, University of California, Berkeley, CA 94720, USA
[e] National Center for Agro Meteorology, Seoul 08826, South Korea
[f] National Institute of Agricultural Sciences, Rural Development Administration, Wanju, 55365, South Korea
[g] Rubber Research Institute (RRI), Chinese Academy of Tropical Agricultural Sciences(CATAS), Hainan Province, 571737, P. R. China
[h] Institute of Geographical Science and Natural Resource Research, Chinese Academy of Sciences, Beijing 100101, China
[i] International Center for Agricultural Research in Dry Areas, Amman, 11195, Jordan

ARTICLE INFO

Article history:
Received 1 April 2016
Received in revised form 28 October 2016
Accepted 30 November 2016
Available online xxxx

Keywords:
Multi-site CO_2 fluxes
Vegetation Photosynthesis Model
Chlorophyll
Light use efficiency

ABSTRACT

Accurate information on the gross primary production (GPP) of paddy rice cropland is critical for assessing and monitoring rice growing conditions. The eddy co-variance technique was used to measure net ecosystem exchange (NEE) of CO_2 between paddy rice croplands and the atmosphere, and the resultant NEE data then partitioned into GPP (GPP_{EC}) and ecosystem respiration. In this study, we first used the GPP_{EC} data from four paddy rice flux tower sites in South Korea, Japan and the USA to evaluate the biophysical performance of three vegetation indices: Normalized Difference Vegetation Index (NDVI); Enhanced Vegetation Index (EVI), and Land Surface Water Index (LSWI) in terms of phenology (crop growing seasons) and GPP_{EC}, which are derived from images taken by Moderate Resolution Imaging Spectroradiometer (MODIS) sensors. We also ran the Vegetation Photosynthesis Model (VPM), which is driven by EVI, LSWI, photosynthetically active radiation (PAR) and air temperature, to estimate GPP over multiple years at these four sites (GPP_{VPM}). The 14 site-years of simulations show that the seasonal dynamics of GPP_{VPM} successfully tracked the seasonal dynamics of GPP_{EC} ($R^2 > 0.88$ or higher). The cross-site comparison also shows that GPP_{VPM} agreed reasonably well with the variations of GPP_{EC} across both years and sites. The simulation results clearly demonstrate the potential of the VPM model and MODIS images for estimating GPP of paddy rice croplands in the monsoon climates of South Korea and Japan and the Mediterranean climate in California, USA. The application of VPM to regional simulations in the near future may provide crucial GPP data to support the studies of food security and cropland carbon cycle around the world.

1. Introduction

Paddy rice is a very important grain crop, comprising about 163 million ha worldwide in 2014 – an 11% increase over the past ten years (FAOSTAT, 2015). Asia provides the world's largest rice area and production, accounting for approximately 88% of the globally harvested rice area and 91% of the global rice production in 2014 (FAOSTAT, 2015). Seasonally flooded paddy rice fields are a major source of methane emissions (in the range of 31–112 Tg yr^{-1}), amounting to 12–26% of the anthropogenic CH_4 release (Gutierrez et al., 2013; Ly et al., 2013; Tokida et al., 2010) and contributing about 11% of the total methane flux to the atmosphere (Allen et al., 2003; Dentener and Raes, 2002; Li et al., 2005; Prather and Ehhalt, 2001). Although several *in-situ* studies reported that paddy rice fields had high soil carbon sequestration and acted as net sinks for CO_2 (Bhattacharyya et al., 2014; Kell, 2012; Liu et al., 2013; Mandal et al., 2007; Pan et al., 2004; Zhang et al., 2014), there are very limited knowledge and large uncertainty about the carbon fluxes of paddy rice fields. Therefore, it is important to measure and model the carbon fluxes of paddy rice fields, including the net ecosystem exchange (NEE) of CO_2 between paddy rice fields and the

* Corresponding author at: Department of Microbiology and Plant Biology, Center for Spatial Analysis, University of Oklahoma, Norman, OK 73019, USA.
E-mail address: xiangming.xiao@ou.edu (X. Xiao).

http://dx.doi.org/10.1016/j.rse.2016.11.025

atmosphere, gross primary production (GPP), and ecosystem respiration (ER) across the diverse climate, soils and crop production systems.

The eddy covariance (EC) technique has been used to measure the net ecosystem exchange of CO_2 between the land surface and the atmosphere over various biomes, and the observed NEE data then partitioned into GPP and ER (Baldocchi et al., 2001). The observed NEE data and derived GPP and ER data from CO_2 flux tower sites have been widely used to support model development and satellite remote sensing across local, regional and global scales (Mahadevan et al., 2008; Running et al., 1999; Stockli et al., 2008; Williams et al., 2009). Out of hundreds of CO_2 eddy flux tower sites in operation, however, there are only a few CO_2 flux tower sites that measure carbon fluxes over paddy rice ecosystems (Alberto et al., 2012; Alberto et al., 2009; Baldocchi et al., 2001; Bhattacharyya et al., 2013; Chen et al., 2015; Hatala et al., 2012; Hossen et al., 2012; Knox et al., 2015; Matthes et al., 2015; Mizoguchi et al., 2009; Ono et al., 2015; Ren et al., 2007; Rossini et al., 2010; Saito et al., 2005; Yang et al., 2016).

Remote sensing provides another viable way to measure the structure and function of terrestrial ecosystems and scale-up carbon fluxes from local to regional and global scales. A number of light (radiation) use efficiency (LUE) models, sometimes called production efficiency models (PEM), have been developed to estimate GPP of terrestrial ecosystems, driven by vegetation indices (VI) derived from optical images and climate data (Barton and North, 2001; Brogaard et al., 2005; Machwitz et al., 2015; Nichol et al., 2000; Seaquist et al., 2003; Yuan et al., 2007). These models estimate GPP as a product of absorbed photosynthetically active radiation (APAR) and light use efficiency (ε) ($GPP = APAR \times \varepsilon$) and can be divided into two groups depending on their approaches to estimate APAR (Dong et al., 2015). One group of LUE models uses the fraction of photosynthetically active radiation (PAR) absorbed by the vegetation canopy ($FPAR_{canopy}$) to estimate $APAR_{canopy}$ ($APAR_{canopy} = PAR \times FPAR_{canopy}$), including the Global Production Efficiency Model (GloPEM) (Prince, 1995), Carnegie-Ames-Stanford Approach (CASA) model (Potter, 1999; Potter et al., 1993), and Photosynthesis (PSN) model (Running et al., 2000; Zhao et al., 2005). The other group of LUE models uses the fraction of PAR absorbed by chlorophyll or green leaves ($FPAR_{chl}$ or $FPAR_{green}$) to estimate $APAR_{chl}$ ($APAR_{chl} = PAR \times FPAR_{chl}$) (Gitelson et al., 2006; Sims et al., 2006; Wu et al., 2010; Xiao et al., 2004b; Zhang et al., 2013; Zhang et al., 2009; Zhang et al., 2006). The Vegetation Photosynthesis Model (VPM) is the first GPP model that uses $FPAR_{chl}$ concept to estimate $APAR_{chl}$ and GPP (Xiao et al., 2004a). The VPM model has been applied to estimate GPP over a variety of CO_2 flux tower sites, including forests (temperate deciduous broadleaf forest, evergreen coniferous forest, seasonally moist tropical forest) (Xiao et al., 2004a; Xiao et al., 2004b; Xiao et al., 2005a; Xiao et al., 2005b), savannas(Jin et al., 2013), grasslands (Li et al., 2007; Wagle et al., 2014; Wu et al., 2008), upland crops (maize, winter wheat, soybean) (Kalfas et al., 2011; Wang et al., 2010), and freshwater inland wetlands (Kang et al., 2014b). However, it has not yet been applied to estimate GPP of paddy rice fields. Given the important role of paddy rice fields in food security, climate and hydrology, individual site verification of the VPM model is critical prior to its usage at the regional and global scales.

The objectives of this study are twofold: (1) to evaluate the biophysical performance of vegetation indices in paddy rice fields, including Normalized Difference Vegetation Index (NDVI), Enhanced Vegetation Index (EVI) and Land Surface Water Index (LSWI); and (2) to apply and assess the VPM estimates of GPP of paddy rice fields over multiple years. Based on the availability of in-situ data from CO_2 eddy flux tower sites, we selected two paddy rice sites in South Korea, one site in Japan, and one site in California, USA. These four sites represent two different climate systems (monsoon climate in eastern Asia and Mediterranean climate in California) and cropping practices (single paddy rice crop, barley-rice double cropping rotation in a year, and a mix of paddy rice and natural wetlands). The results of this work may offer significant contribution to the improvement of GPP models and our long-term capacity for monitoring the paddy rice agriculture that feeds >50% of the world's human population.

2. Materials and methods

2.1. Description of the study sites

In this study we selected four paddy rice flux tower sites (Table 1): Gimje site and KoFlux Haenam site in South Korea, Mase site in Japan, and the Twitchell Island site in California, USA (Fig. 1). Detailed descriptions of these four sites can be obtained via the websites for AmeriFlux (http://ameriflux-data.lbl.gov:8080/SitePages/siteInfo.aspx?US-Twt) and AsiaFlux (http://asiaflux.net/?page_id=22). The flux footprint analysis of the four flux tower sites can be found in the Supplementary Information SI. Here we provide a brief description of these sites (Table 1).

2.1.1. The Gimje paddy rice site in South Korea (GRK)

The GRK site (35.7451°N, 126.8524°E) is located in the southwestern coastal zone of South Korea, where barley and paddy rice double cropping practices are widely distributed. The flux tower's surrounding area is flat with an elevation of approximately 21 m above sea level; soil types at the site are silt loam. On average, the annual mean air temperature is 12.9 °C and annual precipitation is 1253 mm. The site rotates barley and paddy rice each year: barley is planted in late October of the previous year and harvested in early June, and then rice plants are transplanted in June and harvested in October(Min et al., 2014; Min et al., 2013; Shim et al., 2015).

2.1.2. The Haenam paddy rice site in South Korea (HFK)

The HFK site (34.5538°N, 126.5699°E) is located near the southwestern coastal zone of South Korea, where a variety of land cover types exist, including rice paddies (Kwon et al., 2010; Kwon et al., 2009). The terrain is relatively flat with an elevation of 13.7 m above sea level. On average, the annual mean air temperature is 13.3 °C and annual precipitation is 1306 mm (Ryu et al., 2008). Soil types at the site vary from silt loam to loam. The site has a two-crop rotation (other crop-rice) in a year. The fields are flooded in late May, and rice plants transplanted in early-July and harvested in late-September or early October.

2.1.3. The MASE paddy rice site in Japan (MSE)

The Mase paddy rice site (36.0539°N, 140.0269°E) is located in a rural area of Tsukuba city in central Japan, about 50-km northeast of Tokyo (Saito et al., 2005). The climate is warm and humid. The study site is within irrigated flat rice fields extending 1.5 km (north-south) by 1 km (east-west). On average, annual precipitation is approximately 1236 mm, and the annual mean air temperature is 13.5 °C. Local farmers manage the site as a single-rice cropping paddy field; their cropping practice and calendar is representative of the region. The paddy rice field is plowed and flooded in late April, and rice plant transplanting occurs in early May. Rice plants are harvested in early or mid-September.

2.1.4. The Twitchell island paddy rice site in the USA (TWT)

The Twitchell Island paddy rice site (38.1087°N, 121.6530°W) is owned and managed by the California Department of Water Resources and is within the Sacramento-San Joaquin Delta, approximately 100 km inland from the Pacific Ocean (Knox et al., 2015). Between July 2009 and January 2010, the site was located ~300 m to the South (38.105530°N, 121.652097°W). The region experiences a Mediterranean climate. On average, the annual mean air temperature is 15.6 °C, and annual precipitation is 421 mm. Two varieties of rice were planted from mid-April to May and harvested between late September and October or early November (Hatala et al., 2012; Knox et al., 2016; Knox et al., 2015).

Table 1
The characteristics of the four rice paddy CO_2 eddy flux tower sites (two in South Korea, one in Japan and one in California, USA)

Site name	Country	Latitude (°)	Longitude (°)	Elevation (m)	MAP (mm)	MAT (°C)	Soil type	Data Availability
Gimje	Korea	35.7451	126.8524	21	1253	12.9	Silt Loam	2013
Haenam	Korea	34.5538	126.5699	13.74	1306	13.3	Silt loam to loam	2008–2011
Mase	Japan	36.0539	140.0269	13	1200	13.7	Grayed lowland paddy soil	2003–2005
Twitchell Island	U.S.A.	38.10553 38.1055	−121.652097 −121.6530	−5	421	15.6	Degraded peat silt loam	2009–2010 2011–2014

MAP: mean annual precipitation; MAT: mean annual temperature.

2.2. CO_2 flux and climate data from the flux tower sites

2.2.1. The MASE flux tower site in Japan

Open-path eddy covariance sensors were used to measure CO_2 flux at the flux tower site. Detailed descriptions of the flux tower settings are described in a previous study (Saito et al., 2005). Net ecosystem exchange (NEE) of CO_2 between paddy rice fields and the atmosphere was partitioned into ecosystem respiration (ER) and GPP (Saito et al., 2005). This partitioning uses a conventional method that estimates nighttime ER (nighttime NEE) as an exponential function of air temperature and applies this function to the daytime to estimate daytime ER; GPP is then calculated as the difference between NEE and ER (Saito et al., 2005). The half-hourly CO_2 flux data were aggregated to daily sum of GPP, ER and NEE (g C/m2/day). Daily carbon flux data, PAR data (mol PPFD/m^2/day) and air temperature data (°C) were averaged over an 8-day period (following the MODIS 8-day composites). We used daily and 8-day data from 2003 to 2005 within the plant growing season in this study.

2.2.2. The Gimje site in South Korea

An open-path eddy covariance system was used to measure CO_2 fluxes at this site. Detailed information on flux measurements can be found in Min et al. (2013)(Min et al., 2013). GPP and ER were estimated in the same way as in the Mase site in Japan (Min et al., 2014; Min et al., 2013). Daily GPP, NEE and climate (air temperature and PAR) data from 2013 were averaged over an 8-day period, consistent with MODIS 8-day composite images. We used daily and 8-day data in 2013 within the plant growing season in this study.

2.2.3. The Haenam site in South Korea

An open-path eddy covariance system was used to measure CO_2 flux. The detailed information for flux measurements, data processing, quality control, and gap-filling has been reported in previous publications (Hong et al., 2009; Kang et al., 2014a; Kwon et al., 2010). The missing CO_2 fluxes were estimated using the marginal distribution sampling method (MDS) (Reichstein et al., 2005). For partitioning of NEE flux into gross primary productivity (GPP) and ecosystem respiration (ER), we extrapolated nighttime values of ER into the daytime values using the ER equation (Lloyd and Taylor, 1994) with a short-term temperature sensitivity of ER from the nighttime data (Reichstein et al., 2005). Daily GPP, NEE and climate data from 2008 to 2011 were averaged over an 8-day period, consistent with MODIS 8-day composite images. We use daily and 8-day data in 2008–2011 within the plant growing seasons in this study.

2.2.4. The Twitchell island flux tower in USA

An open-path eddy covariance sensor was used to measure CO_2 fluxes at the flux tower site. The flux tower data were downloaded

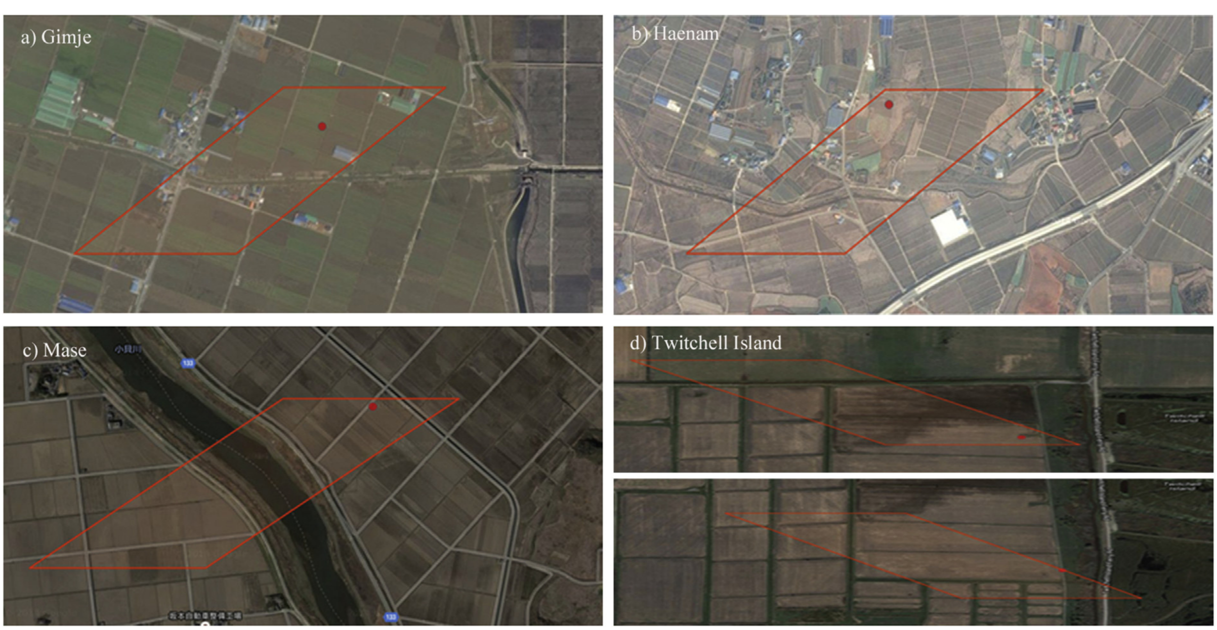

Fig. 1. The landscapes surrounding the locations of the four rice paddy CO_2 eddy flux tower sites (red dots) within a MODIS pixel at the 500 m spatial resolution (red box). (a) Gimje site, South Korea; (b) Haenam site, South Korea; (c) Mase site, Japan; (d) Twitchell Island site, USA. (For interpretation of the references to color in this figure legend, the reader is referred to the web version of this article.)

from the AmeriFlux web site (http://ameriflux.ornl.gov/). Half-hourly fluxes were gap-filled using an artificial neural network (ANN) method as described in Knox et al. (2016). CO_2 fluxes were gap-filled separately for daytime and nighttime observations. Predictions from the ANN resulting from the nighttime gap-filing were used to model ER for all data (daytime and nighttime values) and GPP was calculated by subtracting gap-filled NEE from modeled ER (Baldocchi et al., 2015; Knox et al., 2016). Daily GPP, NEE and climate data from 2009 to 2014 were averaged over an 8-day period, consistent with MODIS 8-day composite images. We use daily and 8-day data in 2009–2014 within the plant growing seasons in this study.

2.3. MODIS imagery and vegetation indices

The MODIS sensor onboard the NASA Terra satellite was launched in December 1999. Out of the 36 spectral bands in the MODIS sensor, seven spectral bands are designed primarily for the study of vegetation and land surface: blue (459–479 nm), green (545–565 nm), red (620–670 nm), near infrared (841–875 m, 1230–1250 nm), and shortwave infrared (1628–1652 nm, 2105–2155 nm). The MODIS sensor acquires daily images at a spatial resolution of 250 m for red and near infrared bands and at a spatial resolution of 500 m for blue, green, near infrared and shortwave infrared bands. The MODIS Land Science Team provides the 8-day Land Surface Reflectance product (MOD09A1) at a 500-m spatial resolution to the public.

Based on the geo-location information (latitude and longitude) of individual CO_2 flux tower sites, time series data of land surface reflectance and quality flags in the MOD09A1 files were extracted from one MODIS pixel where the flux towers are geo-located. The footprint size of a CO_2 flux tower is often comparable with the spatial resolution (500-m) of a MODIS pixel. Bad-quality observations were gap-filled using the three-step procedure (Jin et al., 2013). The three vegetation indices were calculated by using 8-day composite surface reflectance data from the blue, green, red, NIR1, and SWIR1 bands (Eq. (1)–(3)): (1) Normalized Difference Vegetation Index (NDVI; (Tucker, 1979)), (2) Enhanced Vegetation Index (EVI; (Huete et al., 2002; Huete et al., 1997)), and (3) Land Surface Water Index (LSWI; (Xiao et al., 2002)).

$$NDVI = \frac{\rho_{NIR} - \rho_{Red}}{\rho_{NIR} + \rho_{Red}} \tag{1}$$

$$EVI = 2.5 \times \frac{\rho_{NIR} - \rho_{Red}}{\rho_{NIR} + 6 \times \rho_{Red} - 7.5 \times \rho_{Blue} + 1} \tag{2}$$

$$LSWI = \frac{\rho_{NIR} - \rho_{SWIR}}{\rho_{NIR} + \rho_{SWIR}} \tag{3}$$

2.4. The Vegetation Photosynthesis Model (VPM)

Building upon the concept that a vegetation canopy is composed of chlorophyll (chl) and non-photosynthetic vegetation (NPV) that includes the materials at both canopy-level (e.g., stem, branch, senescent leaves) and leaf-level (e.g., cell walls, vein, and other pigments), the VPM model was developed to estimate gross primary production over the photosynthetically active period of vegetation as the product of (1) amount of photosynthetically active radiation (PAR) absorbed by chlorophyll ($APAR_{chl} = FPAR_{chl} \times PAR$) and light use efficiency (Xiao et al., 2004a). The VPM is described as the following:

$$GPP = \varepsilon_g \times FPAR_{chl} \times PAR \tag{4}$$

where ε_g parameter is the light use efficiency for gross primary production (μmol CO_2/μmol PPFD), and PAR is the photosynthetically active radiation (μmol photosynthetic photon flux density, PPFD). $FPAR_{chl}$ within the photosynthetically active period of vegetation is estimated as a linear function of Enhanced Vegetation Index (EVI), and the coefficient α is set to be 1.0 (Xiao et al., 2004a; Xiao et al., 2004b; Zhang et al., 2016):

$$FPAR_{chl} = \alpha \times EVI \tag{5}$$

Light use efficiency (ε_g) is affected by temperature and water and can be expressed as:

$$\varepsilon_g = \varepsilon_0 \times T_{scalar} \times W_{scalar} \tag{6}$$

where ε_0 is the apparent quantum yield or maximum light use efficiency (μmol CO_2/μmol PPFD, or g C/mol PPFD), and T_{scalar} and W_{scalar} are the scalars for the effects of temperature and water on light use efficiency of vegetation, respectively. Ecosystem-level ε_0 values can be obtained from analysis of net ecosystem exchange (NEE) of CO_2 and incident PAR (μmol/m^2/s) at CO_2 eddy flux tower sites, either by using the hyperbolic light response function (Goulden et al., 1997) or from the literature. In this study, the ecosystem-level ε_0 value was set to be 0.6 g C/mol PPFD (0.05 mol CO_2/mol PPFD) based on analyses of half-hourly NEE and incident PAR data at the Mase site, Japan, during the peak growing season; this value is smaller than those based on GPP and absorbed PAR by rice plant canopy (Saito et al., 2005).The effect of temperature on photosynthesis (T_{scalar}) is estimated at each time step using the equation developed for the Terrestrial Ecosystem Model (Raich et al., 1991):

$$T_{scalar} = \frac{(T - T_{min})(T - T_{max})}{[(T - T_{min})(T - T_{max})] - (T - T_{opt})^2} \tag{7}$$

T_{max} and T_{opt} are minimum, maximum and optimal temperature for photosynthetic activities, respectively. In this study, the T_{min} and T_{max} of all the sites were set to be 0 °C (cold damage to plants) and 48 °C (heat damage to plants), following the parameters for a grassland biome in the Terrestrial Ecosystem Model (Zhang et al., 2016). A recent literature review paper highlights the temperature acclimation and adaptation of photosynthesis for C3 and C4 plants (Yamori et al., 2014). In this study, we investigated the relationship between air temperature and vegetation indices and gross primary production and then selected site-specific T_{opt} parameter values for each of the rice flux tower sites. According to the results from such analyses of these three variables, T_{opt} value was approximately ~25 °C at the two South Korea sites, ~20 °C at the Japan site, and ~18 °C at the USA site (see the Results section for more details).

W_{scalar}, the effect of water on plant photosynthesis, was estimated using satellite-derived Land Surface Water Index (LSWI):

$$W_{scalar} = \frac{1 + LSWI}{1 + LSWI_{max}} \tag{8}$$

where $LSWI_{max}$ is the maximum LSWI during the growing season for individual pixels based on the analysis of LSWI seasonal dynamics derived from MODIS image data. The maximum LSWI value within the plant growing season was used as an approximation of $LSWI_{max}$.

3. Results

3.1. Key rice crop phenological characteristics from seasonal dynamics of climate, vegetation indices, and gross primary production

Fig. 2 shows a comparison of air temperature and PAR across the four sites over several years. The seasonal dynamics of PAR among the four sites are similar with the highest values in mid-summer, except for the KoFlux Haenam site, which experienced frequent cloud cover in summer (Kang et al., 2009; Kwon et al., 2010). The seasonal dynamics of air temperature among the four sites are also similar with the highest values in mid-summer. The plant growing season of paddy rice starts when daily mean temperature reaches 10 °C and above.

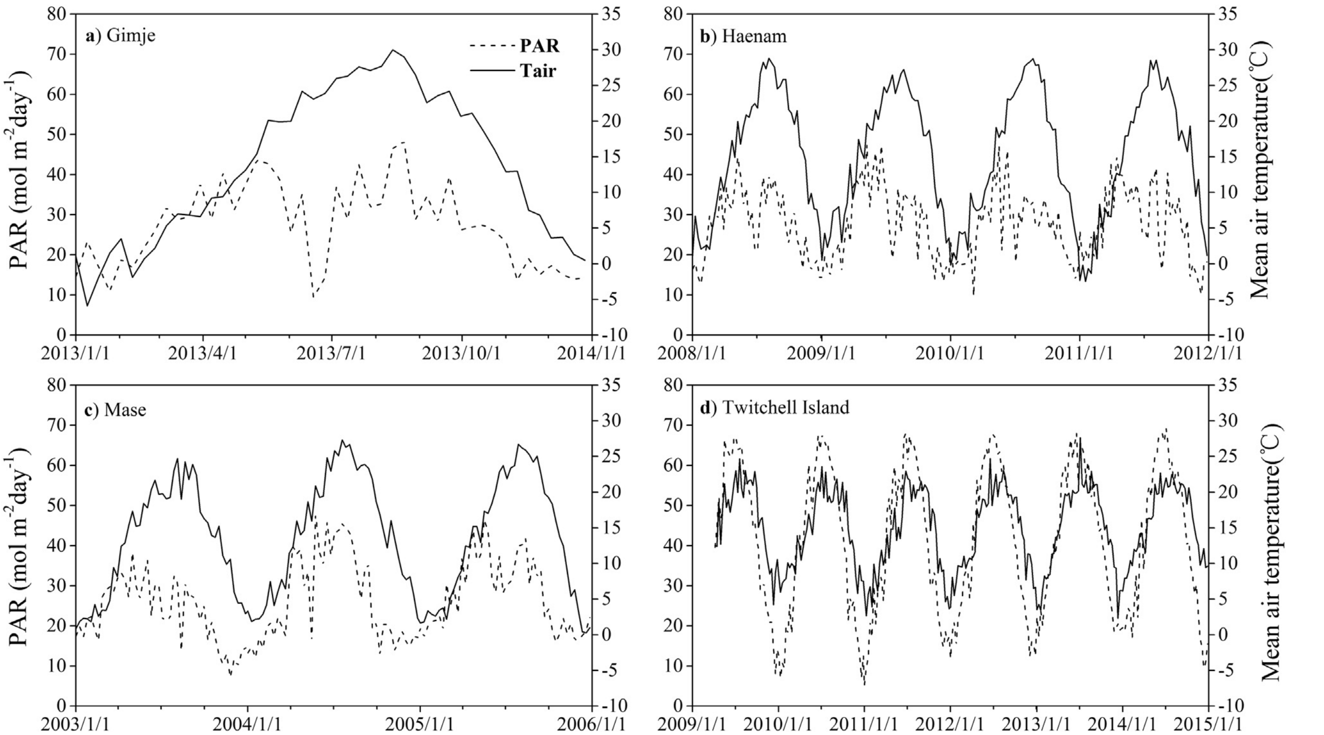

Fig. 2. Seasonal dynamics of photosynthetically active radiation (PAR), air temperature (Tair), estimated GPP (GPP_{EC}) from flux measurements at the four rice paddy CO_2 eddy flux tower sites. (a) Gimje site, South Korea, 2013; (b) Haenam site, South Korea, 2008–2011; (c) Mase site, Japan, 2003–2005; (d) Twitchell Island site, California, USA, 2009–2014.

Fig. 3 also shows a comparison of GPP among the four sites over years. At the Gimje site and Haenam site in South Korea, rice GPP_{EC} started to increase rapidly in mid-June (1 g C m^{-2} day^{-1} or higher), reached its peak in mid-August, and declined to below 1 g C m^{-2} day^{-1} by late October. The carbon uptake period (CUP) of rice paddy as defined by $GPP_{EC} > 1$ g C m − 2 day^{-1} ranges from mid-June to late October. At the Mase site in Japan, farmers transplanted rice plant seedlings in early May and harvested in mid-September. GPP_{EC}

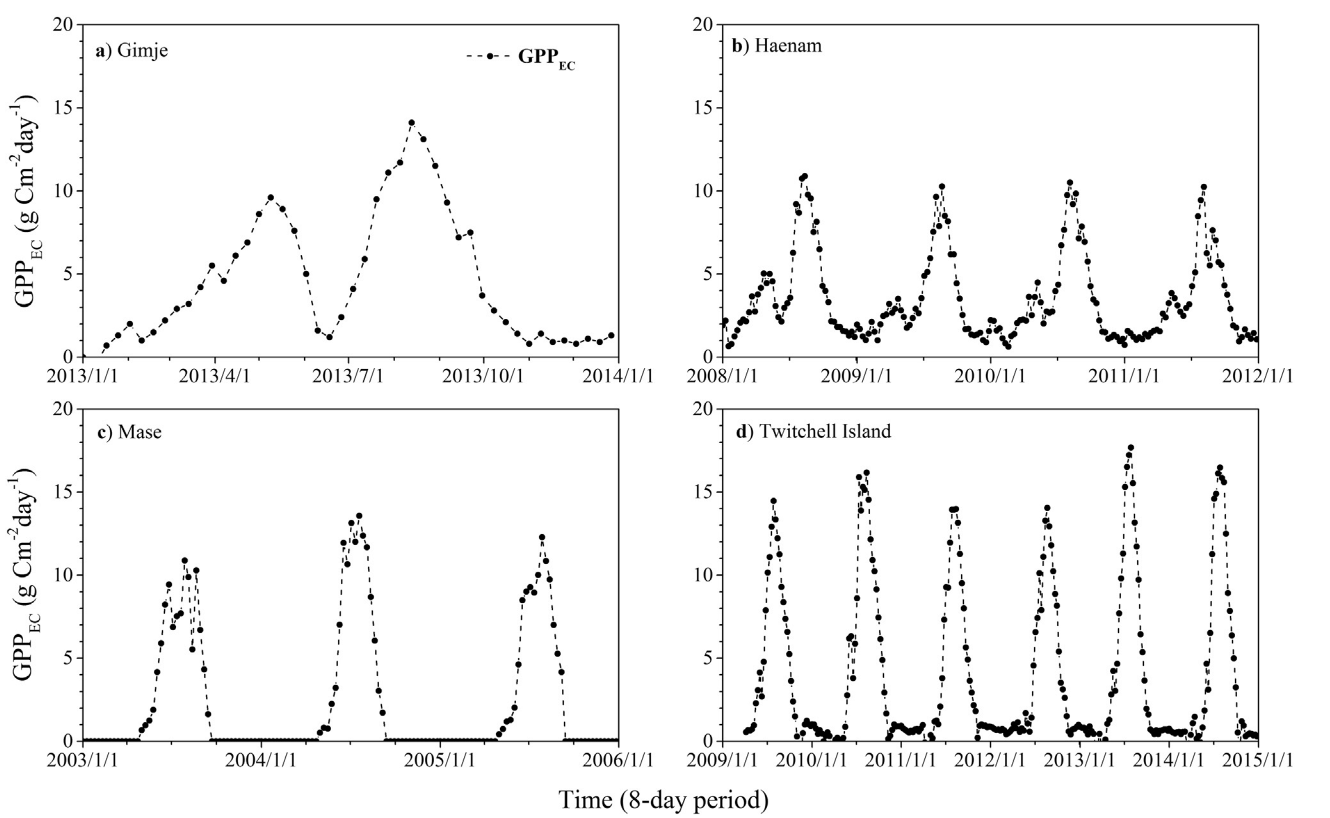

Fig. 3. Seasonal dynamics of estimated GPP (GPP_{EC}) from flux measurements at the four rice paddy CO_2 eddy flux tower sites. (a) Gimje site, South Korea, 2013; (b) Haenam site, South Korea, 2008–2011; (c) Mase site, Japan, 2003–2005; (d) Twitchell Island site, California, USA. 2009–2014.

increased slowly right after rice plant transplanting (GPP_{EC} > 1 g C m^{-2} day^{-1}), reached its peak in late July-early August, and approached zero by September. The carbon uptake period, as delineated by seasonal GPP_{EC}, occurs from early May to September. At the Twitchell Island site, GPP_{EC} (>1 g C m^{-2} day^{-1}) started to increase in May, reached its peak value in August, and decreased to almost zero by late October until harvest. The carbon uptake period as delineated by seasonal GPP_{EC}, occurs from May to October. The daily maximum GPP_{EC} in a year among these four sites (14 site-years) varied between 10 and 20 g C m^{-2} day^{-1} (Fig. 3).

Fig. 4 shows a comparison of the three vegetation indices (NDVI, EVI and LSWI) among the four sites. At the Gimje site, following the harvest of barley in May, the field was flooded and transplanted with rice plants. NDVI and EVI rose rapidly in mid-June, corresponding well with the rapid rise of GPP_{EC} (Fig. 4a). By late October, NDVI, EVI and LSWI reached <0.4, <0.2 and <0.1, respectively, corresponding well with the harvest of paddy rice. Because of the planting and growing of barley (winter/spring crop), both NDVI and EVI increased slightly in November (Fig. 4a). At the Haenam site, NDVI, EVI and LSWI rose rapidly in mid-June and reached <0.4, <0.2, and <0.0, respectively, by late October. At the Mase site, NDVI, EVI and LSWI all rose rapidly in late April and dropped to <0.4, <0.2 and <0.0 by September. At the Twitchell Island site, NDVI, EVI and LSWI rose rapidly in June and dropped to <0.4, <0.2 and <0.0 by October. Among the four sites (14-site-years), the crop growing seasons for rice plants as defined by the seasonal dynamics of vegetation indices are consistent with the GPP_{EC}-based carbon uptake period.

3.2. Temporal correlations between GPP_{EC}, vegetation indices, and air temperature

The relationships between vegetation indices (NDVI and EVI) and GPP_{EC} during the crop growth seasons were plotted for the four sites (Fig. 5). Simple linear regression analyses show that GPP_{EC} has strong linear relationships with both NDVI and EVI; for example, NDVI accounted for 87% of the variance in GPP_{EC} at the Gimje site, 83% at the Haenam site, 75% at the Mase site and 61% at the Twitchell Island site (Fig. 5).

We investigated the relationship between GPP_{EC} and daily mean air temperature (Fig. 6). Rice crops grow well within a daily mean temperature range of 10 to 30 °C. For the three sites in South Korea and Japan, GPP_{EC} increased as temperature rose. For the Twitchell Island site, GPP_{EC} also increased as temperature rose but reached a plateau at approximately 18 °C. This may be related to the Mediterranean climate in California and that cold weather rice cultivars were planted in these years at the site (see (Knox et al., 2016)). At the Mase site, GPP_{EC} started to reach a plateau at ~20 °C (Fig. 6c), and at the Haenam site, GPP_{EC} started to reach a plateau at ~25 °C (Fig. 6b). Based on the canopy physiological analyses of GPP_{EC} and daily mean air temperature at these three sites, these 18, 20, and 25 °C values were then used as the T_{opt} value in the VPM model for the USA, Japan and Korea sites (Table 2). These site-specific variable T_{opt} values are smaller than the biome-specific T_{opt} values (e.g., 27 °C for grasslands and 30 °C for croplands) used in the models (see Table A1 in (Zhang et al., 2016)), and may be related to the acclimation and adaptation of paddy rice to the local thermal environment.

We also investigated the relationship between vegetation indices (NDVI and EVI) and daily mean air temperature (Fig. 7). For the three sites in South Korea and Japan, NDVI and EVI increased as temperature rose. For the Twitchell Island site, NDVI and EVI increased as temperature rose, but clearly reached a peak (plateau) point at approximately 18 °C (Fig. 7d). NDVI and EVI values started to peak at ~20 °C at the Mase site (Fig. 7c) and at 25 °C at the Haenam site (Fig. 7b). The results from the canopy structure analysis (vegetation index – temperature; Fig. 7) at individual sites seems to agree with the results from the canopy physiological analysis (GPP – temperature; Fig. 6) in terms of the

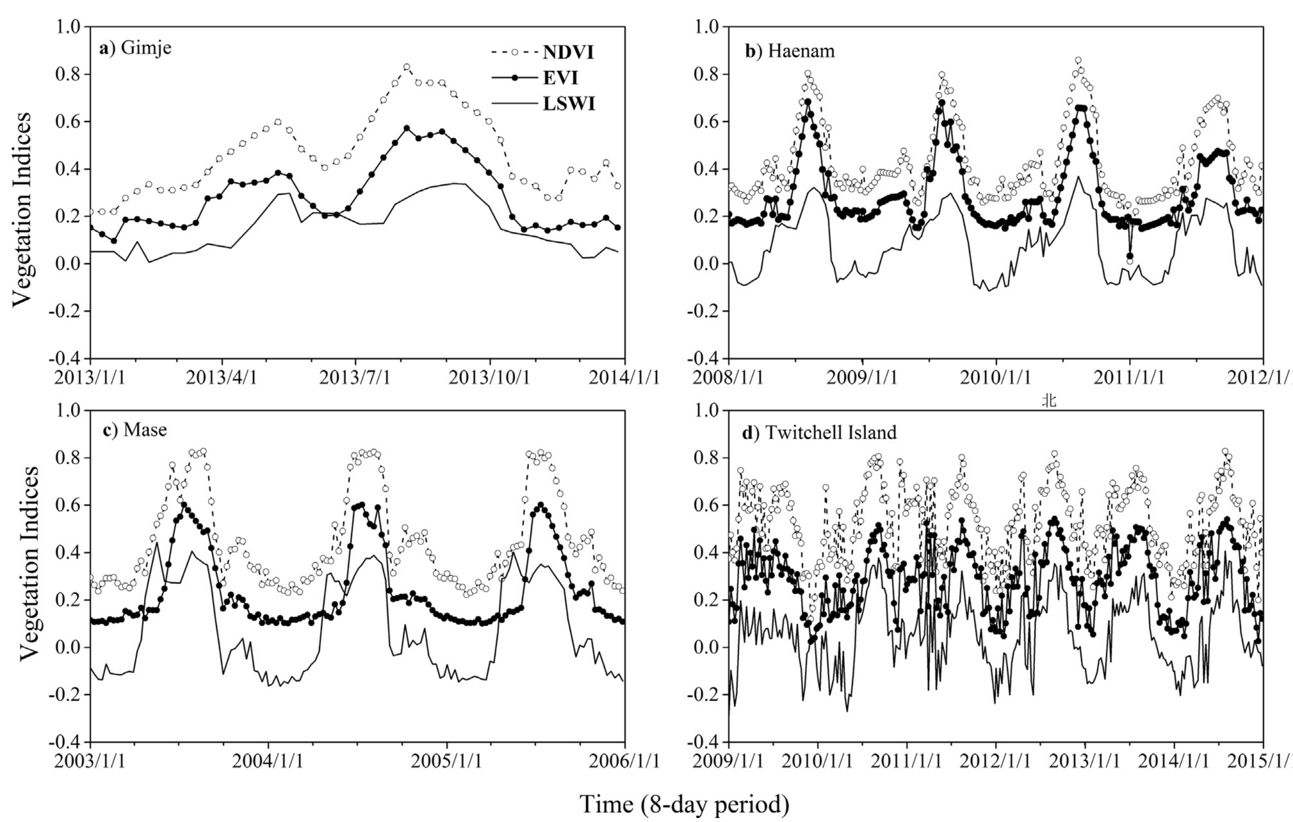

Fig. 4. Seasonal dynamics of three MODIS-derived vegetation indices (NDVI, EVI, and LSWI) at the four rice paddy CO_2 eddy flux tower sites. a) Gimje site, South Korea, 2013; (b) Haenam site, South Korea, 2008–2011; (c) Mase site, Japan, 2003–2005; (d) Twitchell Island site, California, USA, 2009–2014.

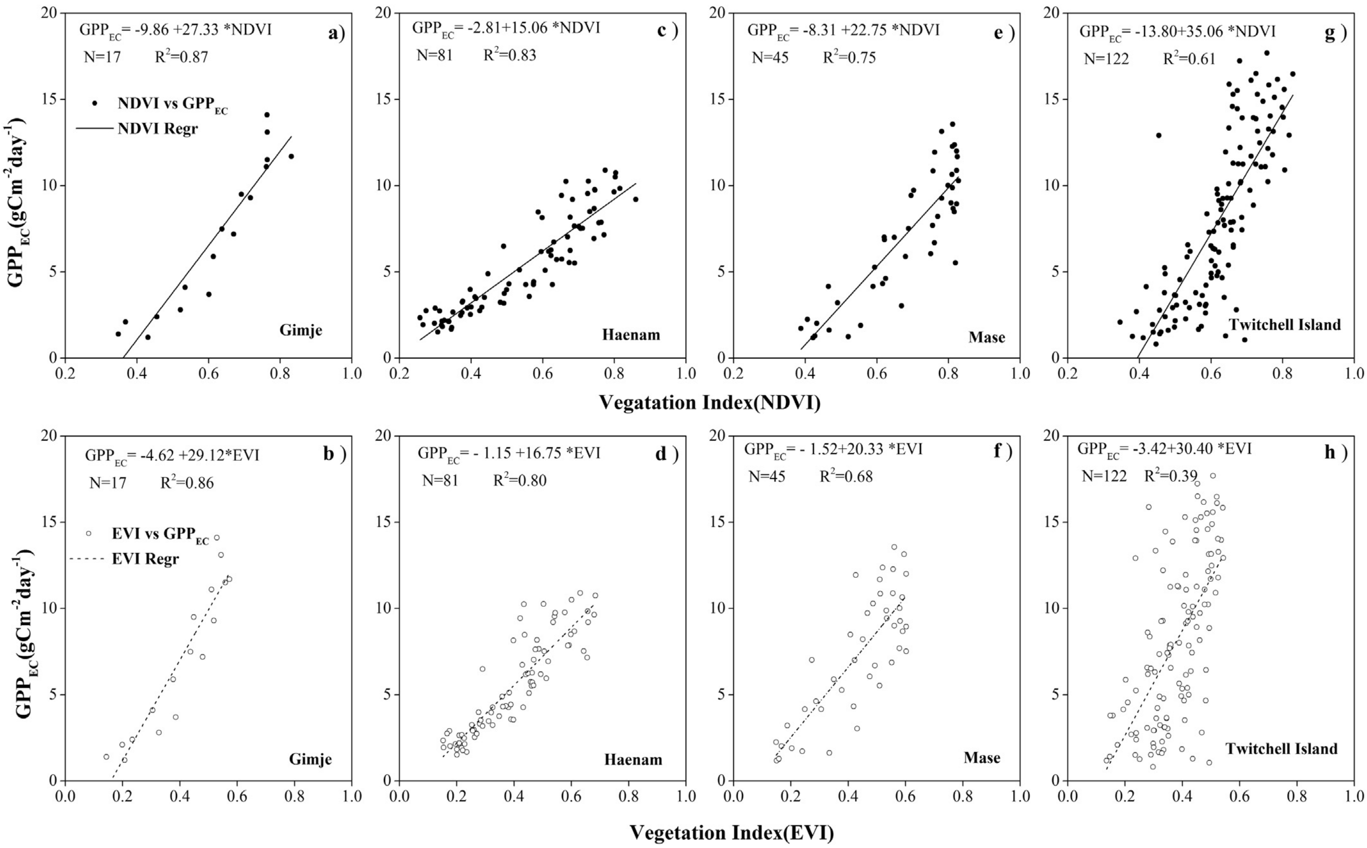

Fig. 5. Relationships between two vegetation indices (NDVI, EVI) and estimated GPP from the flux tower data (GPP_{EC}) during the growing season. (a) and (b) Gimje site, South Korea, 2013; (c) and (d) Haenam site, South Korea, 2008–2011; (e) and (f) Mase site, Japan, 2003–2005; (g) and (h) Twitchell Island site, USA, 2009–2014.

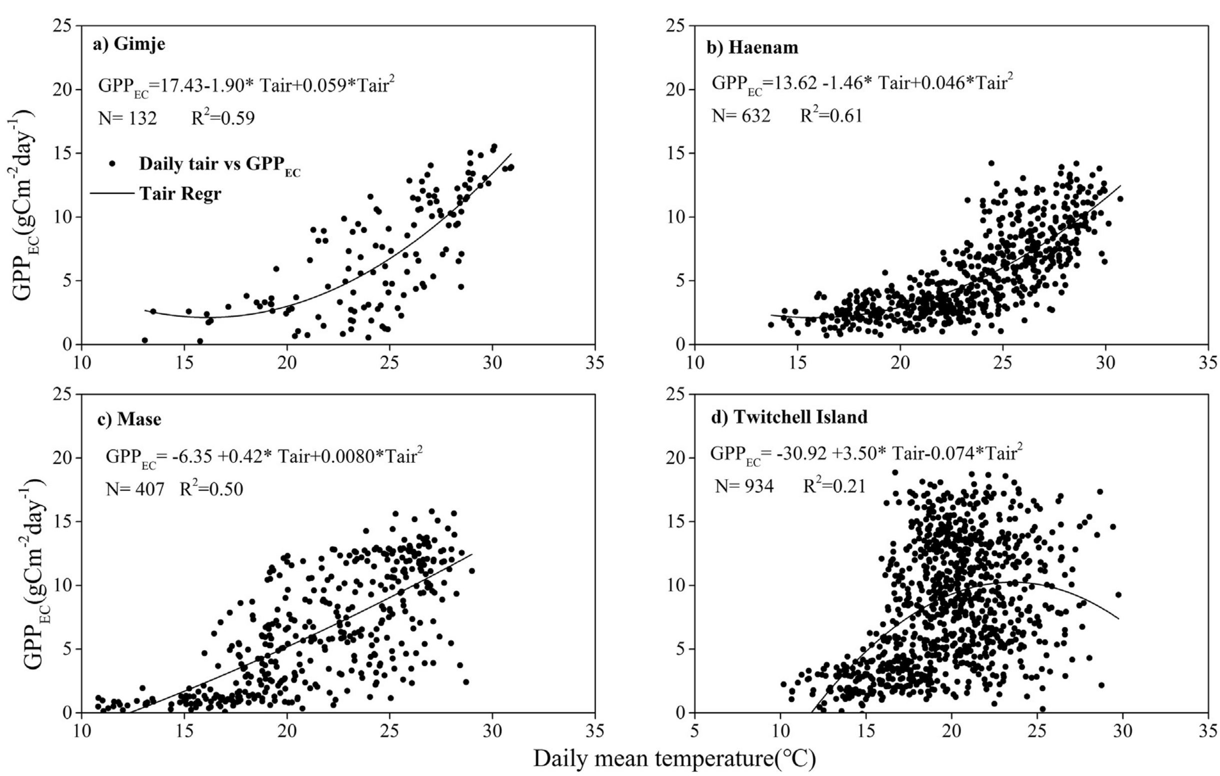

Fig. 6. Relationships between eddy flux measurements estimated GPP (GPP_{EC}) and daily air temperature (Tair) during growing seasons at the four rice paddy CO_2 eddy flux tower sites. (a) Gimje site, South Korea, 2013; (b) Haenam site, South Korea, 2008–2011; (c) Mase site, Japan, 2003–2005; (d) Twitchell Island site, USA, 2009–2014.

Table 2
Parameter values used in the VPM simulations for the four rice sites.

Site/parameter	LUEmax(g C/mol PPFD)	Tmin[a](°C)	Topt[a](°C)	Tmax[a](°C)	LSWImax
Mase, Japan	0.6	0	20	48	0.4440
Gimje, Korea	0.6	0	25	48	0.3390
Haenam, Korea	0.6	0	25	48	0.3690
Twitchell Island, U.S.A	0.6	0	18	48	0.4065

[a] (Raich et al., 1991; Salvucci et al., 2001; Yamori et al., 2014; Zhang et al., 2016) for Tmin, Tmax, Topt respectively.

temperature value at which both GPP and vegetation indices reached certain peak (plateau) values in response to daily mean air temperature during plant growing season. In this study, we introduced the idea of site-specific T_{opt} and assumed that the temperature at the beginning of the plateau in the relationship between GPP_{EC} – temperature would correspond to the optimal temperature values for canopy physiology such as photosynthesis (Table 2), which were used in the VPM simulations (see Section 3.3 for more details). The observed consistency between GPP-Temperature and VI-Temperature allows us to use the VI-Temperature curves to estimate T_{opt} at a site where there is no GPP data. While this approach needs further evaluation at different sites and biomes, it opens a window of opportunity to new ways of estimating site-specific T_{opt} that could potentially replace biome-specific T_{opt} values in models.

3.3. Seasonal dynamics of GPP as predicted by the VPM model (GPP_{VPM})

The seasonal dynamics of GPP predicted by VPM (GPP_{VPM}) were plotted against the seasonal dynamics of GPP_{EC} derived from individual flux tower sites (14 site-years) (Fig. 8). At the Gimje site in South Korea, GPP_{VPM} rose rapidly in June, reached its peak in August and dropped to <1 g C m^{-2} day^{-1} by late October, which clearly tracks well the seasonal dynamics of GPP_{EC}. At the Haenam site, GPP_{VPM} in 2008–2009 overestimated GPP_{EC} for August–September. At the Mase site in Japan, GPP_{VPM} tracked well both seasonal dynamics and interannual variation of GPP_{EC} across 2003–2005. Relatively moderate differences occurred at the early part of the growing season and the post-harvest period, which could be related to other vegetation types within the 500-m MODIS pixel (Fig. 1). At the Twitchell Island site, GPP_{VPM} in 2009 and 2010 agreed well with GPP_{EC} in terms of seasonal maximum GPP. Daily maximum GPP_{VPM} values were much higher than GPP_{EC} in 2011–2012, but only slightly higher than GPP_{EC} in 2013–2014 (Fig. 8d). Among the four sites, the agreement in the seasonal dynamics between GPP_{VPM} and GPP_{EC} was lowest at the Twitchell Island site, mostly attributable to the differences in 2011–2012.

The scatterplots of GPP_{VPM} and GPP_{EC} over the crop growing seasons show strong linear correlations between GPP_{VPM} and GPP_{EC} among the four paddy rice sites (Fig. 9). The slopes of the linear regression models for GPP_{VPM} and GPP_{EC} indicate a range of error (overestimation) from 1% at the Mase site, to 2% at the Gimje site, 12% at the Twitchell Island site, and 16% at the Haenam site. The correlation coefficient at Twitchell is the lowest among the four sites, and the Twitchell Island site has the largest interannual variation of root mean square error (RMSE) (Fig. 9).

The seasonal sums of GPP at the four sites are controlled by (1) phenology, which can be described by the carbon uptake period (CUP), and (2) plant physiology, which can be described by the maximum daily GPP (GPP_{max}) within the carbon uptake period (Churkina et al., 2005; Xia et al., 2015). Following the methods reported in a previous study (Xia et al., 2015), we obtained the CUP (number of days with $GPP > 1$ g C m^{-2} day^{-1}) and GPP_{max} for individual site-years, and calculated the seasonal sum of GPP (GPP_{sum}) and the product of CUP and

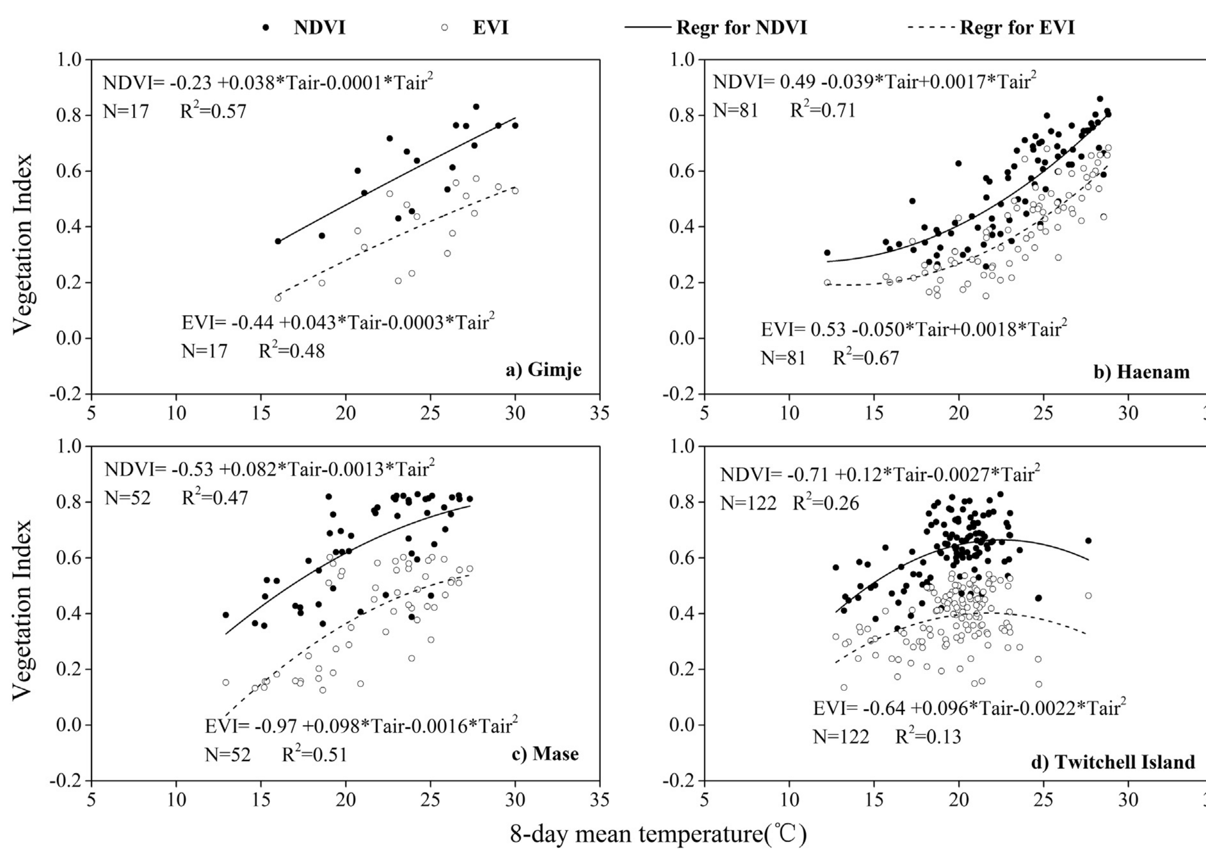

Fig. 7. Scatter plots between air temperature and the vegetation indices (EVI and NDVI) during growing seasons at the four rice paddy CO_2 eddy flux tower sites. (a) Gimje site, South Korea, 2013; (b) Haenam site, South Korea, 2008–2011; (c) Mase site, Japan, 2003–2005; (d) Twitchell Island site, USA, 2009–2014.

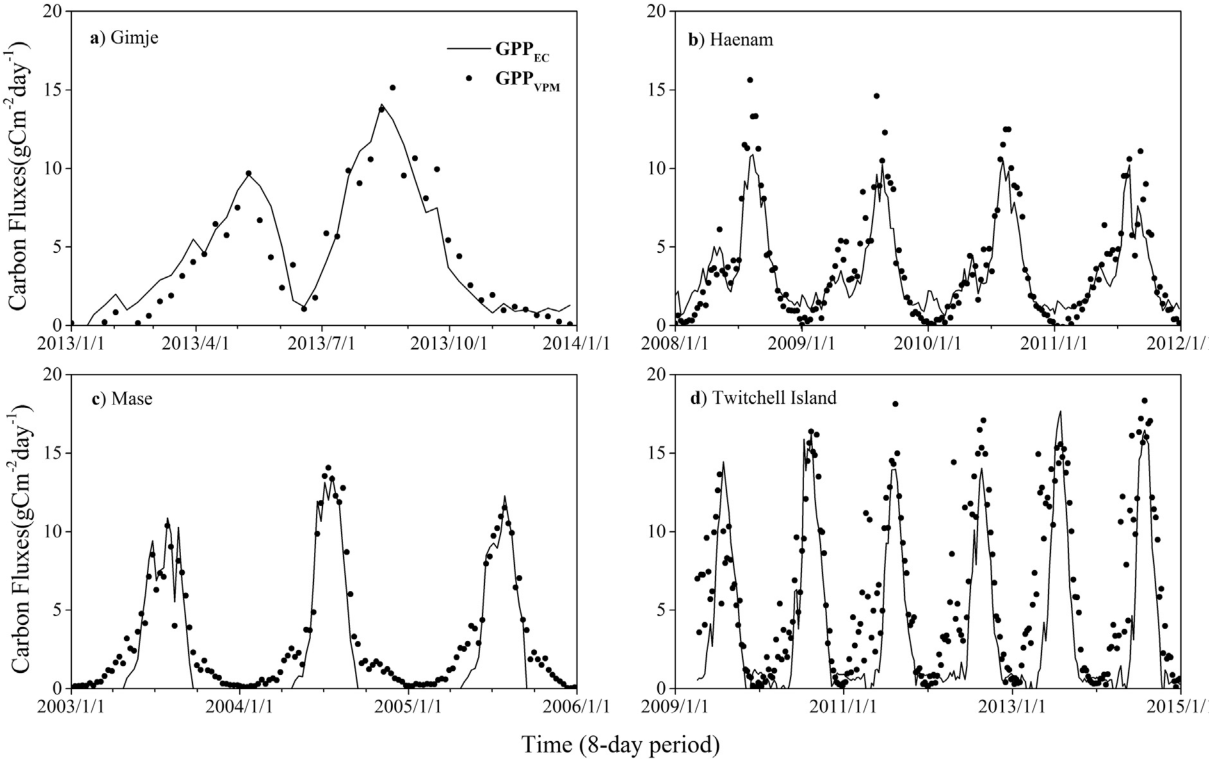

Fig. 8. Seasonal dynamics of predicted and estimated GPP (GPP_{VPM} and GPP_{EC}) at the four rice paddy CO_2 eddy flux tower sites. (a) Gimje site, South Korea, 2013; (b) Haenam site, South Korea, 2008–2011; (c) Mase site, Japan, 2003–2005; (d) Twitchell Island site, USA, 2009–2014.

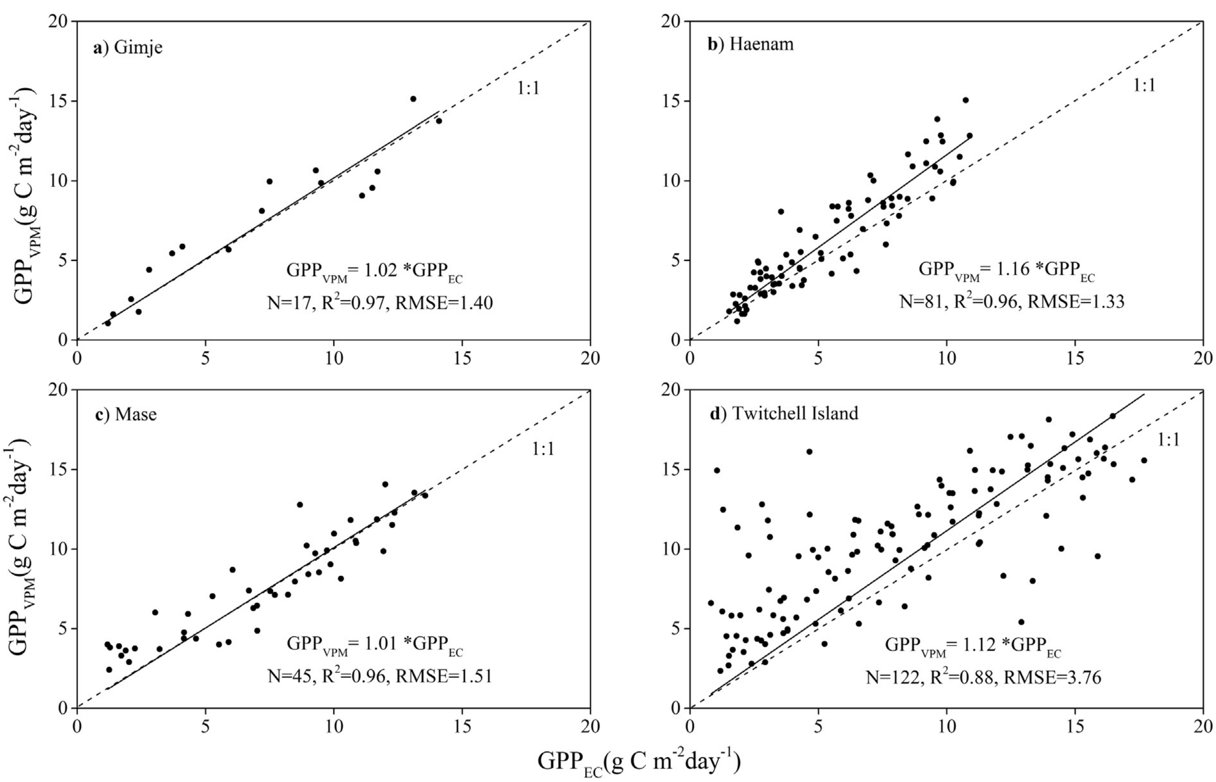

Fig. 9. The comparison between predicted and estimated GPP (GPP_{VPM} and GPP_{EC}) during growing seasons at the four rice paddy CO_2 eddy flux tower sites. (a) Gimje site, South Korea, 2013; (b) Haenam site, Korea, 2008–2011; (c) Mase site, Japan, 2003–2005; (d) Twitchell Island site, USA, 2009–2014. We also report linear regression models with an intercept: (1) Gimje site, $GPP_{VPM} = 0.92 * GPP_{EC} + 0.93$, $R^2 = 0.90$, $N = 17$; (2) Haenam site, $GPP_{VPM} = 1.13 * GPP_{EC} + 0.23$, $R^2 = 0.85$, $N = 17$; (3) Mase site, $GPP_{VPM} = 0.82 * GPP_{EC} + 1.68$, $R^2 = 0.84$, $N = 17$; (4) Twitchell site, $GPP_{VPM} = 0.66 * GPP_{EC} + 4.97$, $R^2 = 0.56$, $N = 17$(see Supplementary Fig. S3).

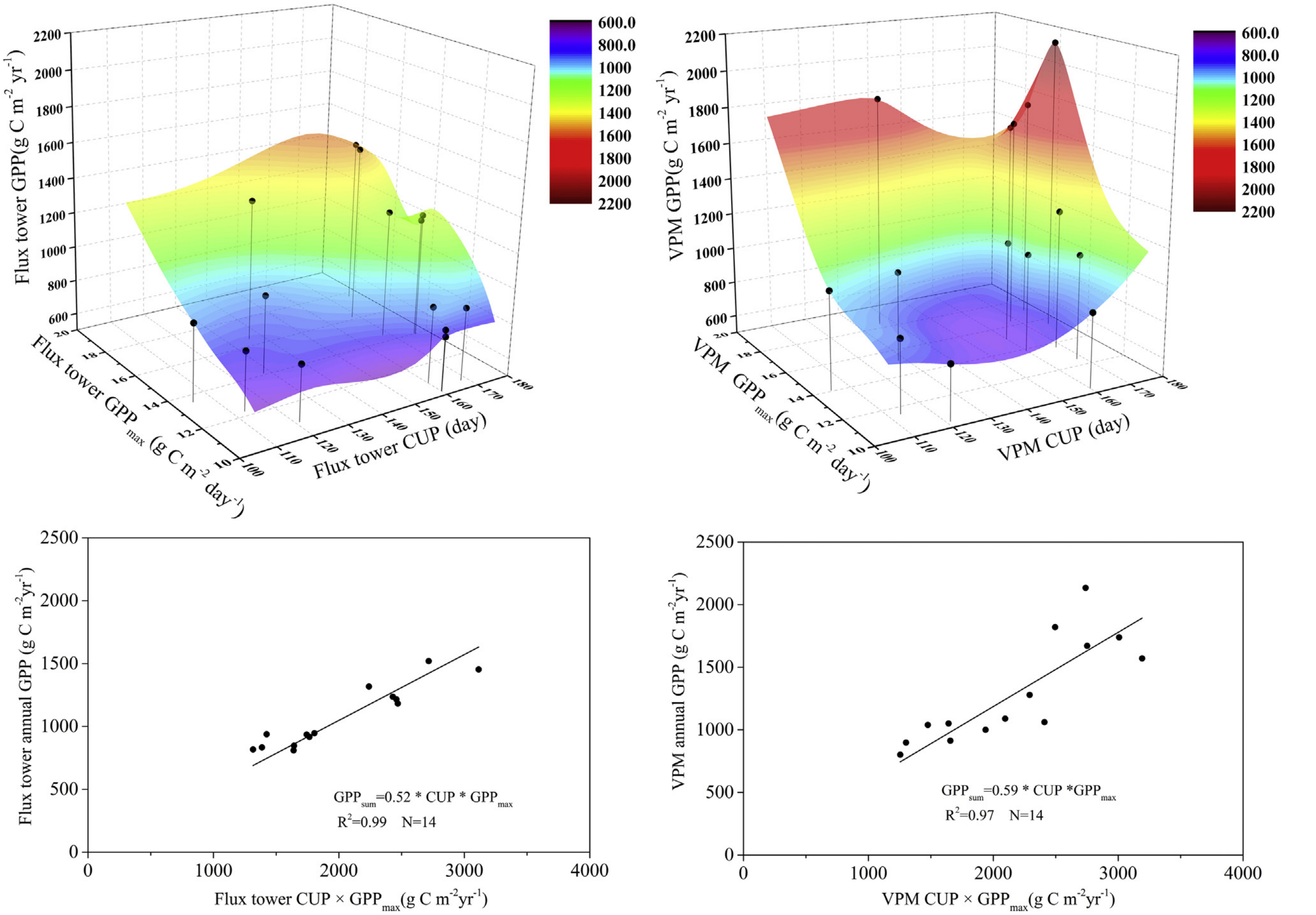

Fig. 10. Joint control of the seasonal sum of GPP by phenology (carbon uptake period, CUP; days) and physiology (maximum daily GPP, GPP_{max}) at the four rice paddy CO_2 eddy flux tower sites. We also report linear regression models with an intercept: (1) for GPP_{EC}, $GPP_{sum} = 0.41 * CUP * GPP_{max} + 276.31$, $R^2 = 0.87$, N = 14; (2) for GPP_{VPM}, $GPP_{sum} = 0.54 * CUP * GPP_{max} + 121.27$, $R^2 = 0.66$, N = 14 (see Supplementary Fig. S4).

GPP_{max} for both GPP_{EC} and GPP_{VPM} at the four sites (14 site-years). As shown in Fig. 10, the seasonal sum of GPP (GPP_{sum}) had strong linear relationships with the product of CUP and GPP_{max} for all the paddy rice site-years. CUP × GPP_{max} explained approximately 99% and 97% of the spatiotemporal variability of GPP at the four sites, respectively. The slope values between GPP_{sum} and the product of CUP × GPP_{max} are 0.524 for GPP_{EC} and 0.593 for GPP_{VPM}, very similar values. The results suggest that both plant phenology and physiology interact to jointly control the gross primary production of paddy rice fields.

4. Discussion

4.1. Biophysical performance of vegetation indices in paddy rice fields

The biophysical performance of greenness-related vegetation indices (NDVI and EVI) can be evaluated by examining the relationships between vegetation indices and GPP during the plant growing seasons at the CO_2 eddy flux tower sites. The results from a number of previous studies showed that EVI has stronger linear relationship with GPP than does NDVI in forests (Xiao et al., 2004a; Xiao et al., 2004b; Xiao et al., 2005a), upland crops (winter wheat, corn, and soybean) (Kalfas et al., 2011; Wagle et al., 2015; Yan et al., 2009), grasslands (Li et al., 2007), and inland freshwater wetlands (Kang et al., 2014b). However, in this study of four paddy rice fields, which are often considered man-made freshwater wetlands and crops, the regression model analyses between vegetation indices and GPP_{EC} showed that both NDVI and EVI have similar linear relationships with the seasonal dynamics of GPP_{EC} (Fig. 5). One reason might be that NDVI in these four paddy rice sites does not yet experience a saturation problem, as most of NDVI values in those site-years are 0.8 or lower. The second reason might be that paddy rice fields have a layer of water, and the lack of exposed soil prevents such an effect on surface reflectance for both NDVI and EVI. The results from these four paddy rice sites clearly call for additional data collection and analysis of GPP and vegetation indices in other paddy rice flux tower sites (Alberto et al., 2015; Bhattacharyya et al., 2013) in the near future.

It has been shown that NDVI and EVI track well the phenological changes of rice crops over time (Boschetti et al., 2009; Kim and Yeom, 2015; Li et al., 2014; Motohka et al., 2009; Singh et al., 2006). Our results from the four paddy rice sites also show that plant growing seasons as delineated by NDVI and EVI correspond well with the carbon uptake period (CUP) as delineated by GPP_{EC}, which suggests consistency in tracking land surface phenology between the remote sensing approach that uses vegetation indices and the ecosystem physiology approach that uses CO_2 flux data (Xiao et al., 2009). In addition to NDVI and EVI that use visible and near infrared bands, other recent research indicates that NIR/SWIR-based vegetation indices (LSWI) also have strong potential for tracking seasonal dynamics of vegetation canopy (Kalfas et al., 2011; Singh et al., 2006; Xiao et al., 2002). In those studies, LSWI <0.0 was used as a threshold value to identify late stage senescence or harvest phases. As shown in Fig. 4, such simple algorithms seem to work well in identifying the harvest phase at the Mase site, Haenam site, and the Twitchell Island site, but fails to work at the Gimje sites, where barley crop was cultivated right after the harvest of paddy rice

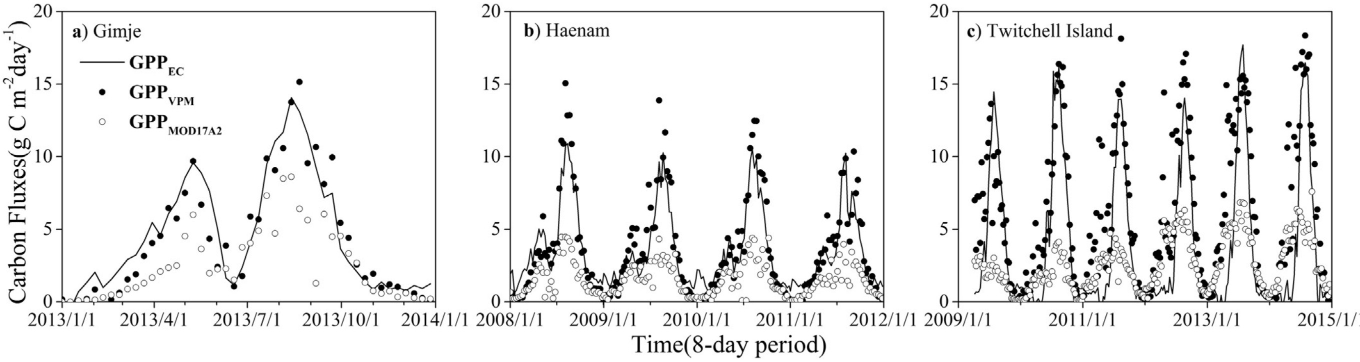

Fig. 11. A comparison of seasonal GPP estimated and predicted from rice paddy CO_2 eddy flux tower, VPM model, and MODIS global GPP data product (GPP_{EC}, GPP_{VPM} and $GPP_{MOD17A2}$) at the rice paddy CO_2 eddy tower sites. (a) Gimje site, South Korea, 2013; (b) Haenam site, South Korea, 2008–2011; (c) Twitchell Island, U.S.A., 2009–2014.

and green-up of those barley crops in the winter season may keep LSWI > 0 (Fig. 4). Therefore, further improvement of the LSWI-based phenology algorithm is needed in the near future.

4.2. A comparison between GPP_{EC}, GPP_{VPM} and GPP from the MOD17A2 data product

A number of light (radiation) use efficiency models have been developed to estimate GPP of terrestrial biomes (Brogaard et al., 2005; Flanagan et al., 2015; He et al., 2013; Ma et al., 2014; Wang et al., 2009; Wu et al., 2012). The MODIS Land Science Team has developed the PSN model and applied it to generate the global GPP data product, namely the Terra/MODIS Gross Primary Productivity (GPP) project (MOD17A2), which is an 8-day composite at a 1-km spatial resolution (Running et al., 2004; Zhao et al., 2006; Zhao et al., 2005). The MOD17A2 product has been applied in many studies of forests, grasslands, and crops (Chen et al., 2014; Christian et al., 2015; Li et al., 2016; Propastin et al., 2012; Tang et al., 2015a; Tang et al., 2015b; Zhao et al., 2006; Zhao and Running, 2010). Recently, a few studies have shown that GPP from the MOD17A2 product underestimates GPP_{EC} (Gitelson et al., 2014; He et al., 2013; Sims et al., 2008; Sjöström et al., 2013). We downloaded the 8-day $GPP_{MOD17A2}$ data (Collection 5) for the Gimje, Haenam and Twitchell Island sites and note that no GPP data are available for the Mase site from the $GPP_{MOD17A2}$ dataset. Fig. 11 shows a comparison of GPP_{EC}, GPP_{VPM} and $GPP_{MOD17A2}$ at the three paddy rice sites. $GPP_{MOD17A2}$ was substantially lower than GPP_{EC} and GPP_{VPM} at the three sites during the plant growing season (Fig. 11). Previous studies also reported that $GPP_{MOD17A2}$ was substantially lower than GPP_{EC} and GPP_{VPM} at savanna and natural wetland sites (Jin et al., 2013; Kang et al., 2014b). The substantial underestimation in $GPP_{MOD17A2}$, relative to GPP_{EC} and GPP_{VPM}, may be attributed to (1) climate data, and (2) the light use efficiency parameter in the model. First, it is well known that climate data determine the seasonality of ecosystem productivity and influence uncertainty of GPP model (Barman et al., 2014; He et al., 2014; Jung et al., 2007; Li et al., 2015; Yuan et al., 2015). There is a possibility that climate data from the global climate dataset, used in the MOD17A2 product, do not match local climate data. Secondly, the light use efficiency parameter is a key parameter in LUE models. There is large uncertainty in estimating the LUE model's maximum light use efficiency (ε_0) parameter, which often varies among models and biome type. In the MOD17A2 data product, the PSN model uses 0.317 g C/mol $PPFD^{-1}$ (0.604 g C MJ^{-1}) as its ε_0 parameter for both croplands and grasslands (see the User's Guide GPP and NPP (MOD17A2/A3) Products, NASA MODIS Land Algorithm). The ε_0 parameter value is the largest uncertainty source of $GPP_{MOD17A2}$. In this study we used a ε_0 parameter value of 0.6 g C/mol $PPFD^{-1}$ for VPM simulations of paddy rice. The comparison between $GPP_{MOD17A2}$ and GPP_{VPM} suggests that additional caution should be taken when using the MOD17A2 product to estimate paddy rice GPP at a regional scale, and that additional evaluation should be done of other paddy rice flux tower sites and additional years for a more comprehensive comparison of GPP_{EC}, GPP_{VPM} and $GPP_{MOD17A2}$.

4.3. Sources of error and uncertainty in VPM simulations of GPP of paddy rice cropland

The results of this study show that the seasonal dynamics of GPP_{VPM} agree reasonably well with GPP_{EC} (Figs. 8 and 9) at the four paddy rice sites (14 site-years), but yielded moderate overestimates at the KoFlux Haenam site (2008–2011) in South Korea and the Twitchell Island site (2011–2014) in California, USA. The moderate overestimates of GPP_{VPM} at the KoFlux Haenam site may be due to the other crops surrounding the rice field, especially in 2009. The overestimates of GPP_{VPM} at the Twitchell Island site could be explained in part by the spatial heterogeneity within the MODIS pixel (see Fig. 1d), with its mix of paddy rice, natural peatland pastures and other upland crops. Paddy rice cultivation was only recently introduced onto Twitchell Island as an agricultural land use to increase carbon storage in the island. The impact of spatial heterogeneity within the MODIS pixels on the comparison between predicted GPP and estimated GPP_{EC} was also evaluated in other studies (Gelybo et al., 2013).

There are a few other error sources relevant to the VPM simulations. The first is the uncertainty of climate data sets such as PAR (Cai et al., 2014; Cheng et al., 2014; He et al., 2014; Ren et al., 2013). The second is the uncertainty of time series vegetation indices derived from various spectral bands, which are affected by many factors such as sun-sensor-object geometry, cloud, cloud shadow, and other atmospheric condition such as aerosols. How to gap-fill and reconstruct vegetation index time series data remains a highly debated research topic. The third lies in the estimation of key parameters in LUE models such as the maximum LUE parameter. It is known and widely assumed that the maximum LUE values at the ecosystem level vary with vegetation types and may even change between different regions of the same ecosystem type (Xiao et al., 2011). In addition, the various estimation methods for the maximum LUE parameter could influence GPP simulations (Sanchez et al., 2015). Two previous in-situ studies estimated maximum LUE in predicting rice yield in Philippine, Italian and Texas, and the resultant maximum LUE parameter varied in the range of 0.977–2.442 g C/mol $PPFD^{-1}$(2–5 g C MJ^{-1}) (Campbell et al., 2001; Kiniry et al., 2001). Another previous study also used a LUE model to estimate rice production in Italy (Boschetti et al., 2011), and the ε_0 parameter value was set to be 1.416 g C/mol $PPFD^{-1}$ (2.9 g C MJ^{-1}). In our study, the maximum LUE of all the four sites in Asia and America was set to 0.6 g C/mol $PPFD^{-1}$. The large range of ε_0 parameter values for croplands evident in the above-mentioned studies clearly suggests that there is a need to evaluate ε_0 parameter values through meta-data analysis of NEE and PAR over most (if not all) paddy rice flux tower sites in the world. A reduction in the uncertainty of the ε_0 value would likely offer substantial improvement in GPP simulations for rice croplands. The fourth source of errors could be the estimation error of tower-based GPP_{EC}. GPP_{EC} is calculated as the difference between modeled ER and measured NEE. In this study, the calculation of GPP_{EC} at these four sites also used different methods, which may have introduced additional uncertainty into the comparison between GPP_{VPM} and GPP_{EC}. The fifth source of errors could be the mismatch in the spatial relationship between the footprint of a CO_2 flux tower (which come in varying sizes and shapes, depending upon the tower height, wind, and land cover types) and a MODIS pixel (500-m spatial resolution; pure or mixed land cover types), which would affect the comparison between GPP_{VPM} and GPP_{EC}.

5. Conclusions

The joint analyses of in-situ flux data (GPP_{EC}) from the eddy flux tower sites and time series of MODIS images at the four paddy rice sites offer insight into the land surface phenology of paddy rice agriculture. GPP_{EC} data from the flux tower sites track land surface phenology from the perspective of ecosystem physiology, and EVI time series from MODIS track land surface phenology from the perspective of ecosystem and landscape structure. The land surface phenology of paddy rice, described by the seasonal dynamics of satellite-derived vegetation indices, is in good agreement with the carbon uptake period (CUP) delineated by seasonal GPP ($GPP_{EC} > 1$) estimates from flux tower sites. The joint analyses of *in-situ* GPP_{EC}, daily mean air temperature and time series MODIS images at the four paddy rice sites also offer insight into the response functions of VI and GPP to daily mean air temperature at the landscape scale. Therefore, additional data analyses are needed in the near future to further evaluate the relationships among GPP_{EC}, daily mean air temperature and vegetation indices at other paddy rice flux tower sites and across more years; such work will improve our capacity to monitor the changes in paddy rice croplands under various climate conditions.

This is the first case study using the Vegetation Photosynthesis Model, which utilizes the concept of light absorption by chlorophyll, to estimate the seasonal dynamics of GPP in paddy rice croplands (single crop and double crops). The results demonstrate that the VPM model performs reasonably well in estimating the seasonal dynamics and inter-annual variation of GPP at the four rice sites, including sites in a monsoon climate in South Korea and Japan and a Mediterranean climate in California, USA. It is important to note that further evaluation of the VPM at other paddy rice sites with CO_2 flux measurements would be valuable and necessary before it is applied to estimate GPP of paddy rice croplands at large scales across different geographic regions around the world. Through systematical study of the scaling-up of the methodology presented in this paper in the near future, the VPM model could potentially become a useful tool for tracking and estimating GPP of paddy rice croplands across the local to nation scales.

Acknowledgements

This data analysis and modeling study was supported in part by grants from NASA Land Use and Land Cover Change program (NNG05GH80G, NNX11AJ35G), NASA Terrestrial Ecology program (NNX010AE103G), NIH NIAID (1R01AI101028-01A1), the International Center for Agriculture in Dry Areas (ICARDA), the California Department of Water Resources (contract # 4600008849), the National Science Foundation (Grant # EF-1241960), the United States Department of Agriculture (NIFA grant #2011-67003-30371), the United States Department of Energy (AmeriFlux contract # 7079856), Korea RDA Research program (PJ122P301), and the Korea Meteorological Administration Weather Information Service Engine (WISE) project (KMIPA-2012-0001). We thank Sarah Xiao at Yale University for English editing of the manuscript. We thank three reviewers for their insightful comments and suggestions on previous versions of manuscript, which help substantilly revision and improvement of this manuscript.

Appendix A. Supplementary data

Supplementary data to this article can be found online at http://dx.doi.org/10.1016/j.rse.2016.11.025.

References

Alberto, M.C.R., Wassmann, R., Hirano, T., Miyata, A., Kumar, A., Padre, A., Amante, M., 2009. CO_2/heat fluxes in rice fields: comparative assessment of flooded and non-flooded fields in the Philippines. Agric. For. Meteorol. 149, 1737–1750.

Alberto, M.C.R., Hirano, T., Miyata, A., Wassmann, R., Kumar, A., Padre, A., Amante, M., 2012. Influence of climate variability on seasonal and interannual variations of ecosystem CO_2 exchange in flooded and non-flooded rice fields in the Philippines. Field Crop Res. 134, 80–94.

Alberto, M.C.R., Wassmann, R., Gummert, M., Buresh, R.J., Quilty, J.R., Correa, T.Q., Centeno, C.A.R., Oca, G.M., 2015. Straw incorporated after mechanized harvesting of irrigated rice affects net emissions of CH_4 and CO_2 based on eddy covariance measurements. Field Crop Res. 184, 162–175.

Allen, L.H., Albrecht, S.L., Colon-Guasp, W., Covell, S.A., Baker, J.T., Pan, D.Y., Boote, K.J., 2003. Methane emissions of rice increased by elevated carbon dioxide and temperature. J. Environ. Qual. 32, 1978–1991.

Baldocchi, D., Falge, E., Gu, L.H., Olson, R., Hollinger, D., Running, S., Anthoni, P., Bernhofer, C., Davis, K., Evans, R., Fuentes, J., Goldstein, A., Katul, G., Law, B., Lee, X.H., Malhi, Y., Meyers, T., Munger, W., Oechel, W., U, K.T.P., Pilegaard, K., Schmid, H.P., Valentini, R., Verma, S., Vesala, T., Wilson, K., Wofsy, S., 2001. FLUXNET: a new tool to study the temporal and spatial variability of ecosystem-scale carbon dioxide, water vapor, and energy flux densities. Bull. Am. Meteorol. Soc. 82, 2415–2434.

Baldocchi, D., Sturtevant, C., Fluxnet, C., 2015. Does day and night sampling reduce spurious correlation between canopy photosynthesis and ecosystem respiration? Agric. For. Meteorol. 207, 117–126.

Barman, R., Jain, A.K., Liang, M.L., 2014. Climate-driven uncertainties in modeling terrestrial gross primary production: a site level to global-scale analysis. Glob. Chang. Biol. 20, 1394–1411.

Barton, C.V.M., North, P.R.J., 2001. Remote sensing of canopy light use efficiency using the photochemical reflectance index—model and sensitivity analysis. Remote Sens. Environ. 78, 264–273.

Bhattacharyya, P., Neogi, S., Roy, K.S., Dash, P.K., Tripathi, R., Rao, K.S., 2013. Net ecosystem CO_2 exchange and carbon cycling in tropical lowland flooded rice ecosystem. Nutr. Cycl. Agroecosyst. 95, 133–144.

Bhattacharyya, P., Neogi, S., Roy, K.S., Dash, P.K., Nayak, A.K., Mohapatra, T., 2014. Tropical low land rice ecosystem is a net carbon sink. Agric. Ecosyst. Environ. 189, 127–135.

Boschetti, M., Stroppiana, D., Brivio, P.A., Bocchi, S., 2009. Multi-year monitoring of rice crop phenology through time series analysis of MODIS images. Int. J. Remote Sens. 30, 4643–4662.

Boschetti, M., Stroppiana, D., Confalonieri, R., Brivio, P.A., Crema, A., Bocchi, S., 2011. Estimation of rice production at regional scale with a Light Use Efficiency model and MODIS time series. Italian J. Remote Sens.-Rivista Italiana Di Telerilevamento 43, 63–81.

Brogaard, S., Runnstrom, M., Seaquist, J.W., 2005. Primary production of Inner Mongolia, China, between 1982 and 1999 estimated by a satellite data-driven light use efficiency model. Glob. Planet. Chang. 45, 313–332.

Cai, W.W., Yuan, W.P., Liang, S.L., Liu, S.G., Dong, W.J., Chen, Y., Liu, D., Zhang, H.C., 2014. Large differences in terrestrial vegetation production derived from satellite-based light use efficiency models. Remote Sens. 6, 8945–8965.

Campbell, C.S., Heilman, J.L., McInnes, K.J., Wilson, L.T., Medley, J.C., Wu, G.W., Cobos, D.R., 2001. Seasonal variation in radiation used efficiency of irrigated rice. Agric. For. Meteorol. 110, 45–54.

Chen, J., Zhang, H., Liu, Z., Che, M., Chen, B., 2014. Evaluating parameter adjustment in the MODIS gross primary production algorithm based on eddy covariance tower measurements. Remote Sens. 6, 3321–3348.

Chen, C., Li, D., Gao, Z.Q., Tang, J.W., Guo, X.F., Wang, L.L., Wan, B.C., 2015. Seasonal and interannual variations of carbon exchange over a rice-wheat rotation system on the north China plain. Adv. Atmos. Sci. 32, 1365–1380.

Cheng, Y.B., Zhang, Q.Y., Lyapustin, A.I., Wang, Y.J., Middleton, E.M., 2014. Impacts of light use efficiency and fPAR parameterization on gross primary production modeling. Agric. For. Meteorol. 189, 187–197.

Christian, B., Joshi, N., Saini, M., Mehta, N., Goroshi, S., Nidamanuri, R.R., Thenkabail, P., Desai, A.R., Krishnayya, N.S.R., 2015. Seasonal variations in phenology and productivity of a tropical dry deciduous forest from MODIS and Hyperion. Agric. For. Meteorol. 214, 91–105.

Churkina, G., Schimel, D., Braswell, B.H., Xiao, X.M., 2005. Spatial analysis of growing season length control over net ecosystem exchange. Glob. Chang. Biol. 11, 1777–1787.

Dentener, F., Raes, F., 2002. Greenhouse gases and atmospheric chemistry: towards integration of air pollution and climate change policies. Non-CO_2 Greenhouse Gases: Scientific Understanding, Control Options and Policy Aspects.

Dong, J., Xiao, X., Wagle, P., Zhang, G., Zhou, Y., Jin, C., Torn, M.S., Meyers, T.P., Suyker, A.E., Wang, J., Yan, H., Biradar, C., Moore, B., 2015. Comparison of four EVI-based models for estimating gross primary production of maize and soybean croplands and tallgrass prairie under severe drought. Remote Sens. Environ. 162, 154–168.

FAOSTAT, 2015. Statistical Database of the Food and Agricultural Organization of the United Nations.

Flanagan, L.B., Sharp, E.J., Gamon, J.A., 2015. Application of the photosynthetic light-use efficiency model in a northern Great Plains grassland. Remote Sens. Environ. 168, 239–251.

Gelybo, G., Barcza, Z., Kern, A., Kljun, N., 2013. Effect of spatial heterogeneity on the validation of remote sensing based GPP estimations. Agric. For. Meteorol. 174, 43–53.
Gitelson, A.A., Vina, A., Verma, S.B., Rundquist, D.C., Arkebauer, T.J., Keydan, G., Leavitt, B., Ciganda, V., Burba, G.G., Suyker, A.E., 2006. Relationship between gross primary production and chlorophyll content in crops: Implications for the synoptic monitoring of vegetation productivity. J. Geophys. Res.-Atmos. 111, 1–13.
Gitelson, A.A., Peng, Y., Arkebauer, T.J., Schepers, J., 2014. Relationships between gross primary production, green LAI, and canopy chlorophyll content in maize: Implications for remote sensing of primary production. Remote Sens. Environ. 144, 65–72.
Goulden, M.L., Daube, B.C., Fan, S.M., Sutton, D.J., Bazzaz, A., Munger, J.W., Wofsy, S.C., 1997. Physiological responses of a black spruce forest to weather. J. Geophys. Res.-Atmos. 102, 28987–28996.
Gutierrez, J., Kim, S.Y., Kim, P.J., 2013. Effect of rice cultivar on CH4 emissions and productivity in Korean paddy soil. Field Crop Res. 146, 16–24.
Hatala, J.A., Detto, M., Sonnentag, O., Deverel, S.J., Verfaillie, J., Baldocchi, D.D., 2012. Greenhouse gas (CO_2, CH_4, H_2O) fluxes from drained and flooded agricultural peatlands in the Sacramento-San Joaquin Delta. Agric. Ecosyst. Environ. 150, 1–18.
He, M.Z., Zhou, Y.L., Ju, W.M., Chen, J.M., Zhang, L., Wang, S.Q., Saigusa, N., Hirata, R., Murayama, S., Liu, Y.B., 2013. Evaluation and improvement of MODIS gross primary productivity in typical forest ecosystems of East Asia based on eddy covariance measurements. J. For. Res. 18, 31–40.
He, H.L., Liu, M., Xiao, X.M., Ren, X.L., Zhang, L., Sun, X.M., Yang, Y.H., Li, Y.N., Zhao, L., Shi, P.L., Du, M.Y., Ma, Y.M., Ma, M.G., Zhang, Y., Yu, G.R., 2014. Large-scale estimation and uncertainty analysis of gross primary production in Tibetan alpine grasslands. J. Geophys. Res. Biogeosci. 119, 466–486.
Hong, J.K., Kwon, H.J., Lim, J.H., Byun, Y.H., Lee, J.H., Kim, J., 2009. Standardization of KoFlux eddy-covariance data processing. Korean J. Agric. For. Meteorol. 11, 19–26.
Hossen, M.S., Mano, M., Miyata, A., Baten, M.A., Hiyama, T., 2012. Surface energy partitioning and evapotranspiration over a double-cropping paddy field in Bangladesh. Hydrol. Process. 26, 1311–1320.
Huete, A.R., Liu, H.Q., Batchily, K., vanLeeuwen, W., 1997. A comparison of vegetation indices global set of TM images for EOS-MODIS. Remote Sens. Environ. 59, 440–451.
Huete, A., Didan, K., Miura, T., Rodriguez, E.P., Gao, X., Ferreira, L.G., 2002. Overview of the radiometric and biophysical performance of the MODIS vegetation indices. Remote Sens. Environ. 83, 195–213.
Jin, C., Xiao, X.M., Merbold, L., Arneth, A., Veenendaal, E., Kutsch, W.L., 2013. Phenology and gross primary production of two dominant savanna woodland ecosystems in Southern Africa. Remote Sens. Environ. 135, 189–201.
Jung, M., Vetter, M., Herold, M., Churkina, G., Reichstein, M., Zaehle, S., Ciais, P., Viovy, N., Bondeau, A., Chen, Y., Trusilova, K., Feser, F., Heimann, M., 2007. Uncertainties of modeling gross primary productivity over Europe: a systematic study on the effects of using different drivers and terrestrial biosphere models. Glob. Biogeochem. Cycles 21, 12.
Kalfas, J.L., Xiao, X.M., Vanegas, D.X., Verma, S.B., Suyker, A.E., 2011. Modeling gross primary production of irrigated and rain-fed maize using MODIS imagery and CO_2 flux tower data. Agric. For. Meteorol. 151, 1514–1528.
Kang, M., Park, S., Kwon, H., Choi, H.T., Choi, Y.J., Kim, J., 2009. Evapotranspiration from a deciduous Forest in a complex terrain and a heterogeneous farmaland under monsoon climate. Asia-Pac. J. Atmos. Sci. 45, 175–191.
Kang, M., Kim, J., Kim, H.-S., Thakuri, B.M., Chun, J.-H., 2014a. On the nighttime correction of CO_2 flux measured by eddy covariance over temperate forests in complex terrain. Korean J. Agric. For. Meteorol. 16, 233–245.
Kang, X., Wang, Y., Chen, H., Tian, J., Cui, X., Rui, Y., Zhong, L., Kardol, P., Hao, Y., Xiao, X., 2014b. Modeling carbon fluxes using multi-temporal MODIS imagery and CO_2 eddy flux tower data in Zoige Alpine Wetland, South-West China. Wetlands 34, 603–618.
Kell, D.B., 2012. Large-scale sequestration of atmospheric carbon via plant roots in natural and agricultural ecosystems: why and how. Philos. Trans. R. Soc. B 367, 1589–1597.
Kim, H.O., Yeom, J.M., 2015. Sensitivity of vegetation indices to spatial degradation of RapidEye imagery for paddy rice detection: a case study of South Korea. Giosci. Remote Sens. 52, 1–17.
Kiniry, J.R., McCauley, G., Xie, Y., Arnold, J.G., 2001. Rice parameters describing crop performance of four US cultivars. Agron. J. 93, 1354–1361.
Knox, S.H., Sturtevant, C., Matthes, J.H., Koteen, L., Verfaillie, J., Baldocchi, D., 2015. Agricultural peatland restoration: effects of land-use change on greenhouse gas (CO_2 and CH_4) fluxes in the Sacramento-San Joaquin Delta. Glob. Chang. Biol. 21, 750–765.
Knox, S.H., Matthes, J.H., Sturtevant, C., Oikawa, P.Y., Verfaillie, J., Baldocchi, D., 2016. Biophysical controls on interannual variability in ecosystem-scale CO_2 and CH_4 exchange in a California rice paddy. J. Geophys. Res. Biogeosci. 121, 978–1001.
Kwon, H., Park, T.-Y., Hong, J., Lim, J.-H., Kim, J., 2009. Seasonality of net ecosystem carbon exchange in two major plant functional types in Korea. Asia-Pac. J. Atmos. Sci. 45, 149–163.
Kwon, H., Kim, J., Hong, J., Lim, J.H., 2010. Influence of the Asian monsoon on net ecosystem carbon exchange in two major ecosystems in Korea. Biogeosciences 7, 1493–1504.
Li, C.S., Frolking, S., Xiao, X.M., Moore, B., Boles, S., Qiu, J.J., Huang, Y., Salas, W., Sass, R., 2005. Modeling impacts of farming management alternatives on CO_2, CH_4, and N_2O emissions: a case study for water management of rice agriculture of China. Glob. Biogeochem. Cycles 19, 13.
Li, Z.Q., Yu, G.R., Xiao, X.M., Li, Y.N., Zhao, X.Q., Ren, C.Y., Zhang, L.M., Fu, Y.L., 2007. Modeling gross primary production of alpine ecosystems in the Tibetan Plateau using MODIS images and climate data. Remote Sens. Environ. 107, 510–519.
Li, S.H., Xiao, J.T., Ni, P., Zhang, J., Wang, H.S., Wang, J.X., 2014. Monitoring paddy rice phenology using time series MODIS data over Jiangxi Province, China. Int. J. Agric. Biol. Eng. 7, 28–36.
Li, D.Q., Ju, W.M., Lu, D.S., Zhou, Y.L., Wang, H.M., 2015. Impact of estimated solar radiation on gross primary productivity simulation in subtropical plantation in southeast China. Sol. Energy 120, 175–186.
Li, S.H., He, P., Liu, B.S., Ni, P., Han, X., 2016. Modeling of maize gross primary production using MODIS imagery and flux tower data. Int. J. Agric. Biol. Eng. 9, 110–118.
Liu, Y., Wan, K.Y., Tao, Y., Li, Z.G., Zhang, G.S., Li, S.L., Chen, F., 2013. Carbon dioxide flux from rice paddy soils in central China: effects of intermittent flooding and draining cycles. PLoS One 8, 8.
Lloyd, J., Taylor, J.A., 1994. On the remperature dependence of soil respiration. Funct. Ecol. 8, 315–323.
Ly, P., Jensen, L.S., Bruun, T.B., de Neergaard, A., 2013. Methane (CH_4) and nitrous oxide (N_2O) emissions from the system of rice intensification (SRI) under a rain-fed lowland rice ecosystem in Cambodia. Nutr. Cycl. Agroecosyst. 97, 13–27.
Ma, X.L., Huete, A., Yu, Q., Restrepo-Coupe, N., Beringer, J., Hutley, L.B., Kanniah, K.D., Cleverly, J., Eamus, D., 2014. Parameterization of an ecosystem light-use-efficiency model for predicting savanna GPP using MODIS EVI. Remote Sens. Environ. 154, 253–271.
Machwitz, M., Gessner, U., Conrad, C., Falk, U., Richters, J., Dech, S., 2015. Modelling the gross primary productivity of West Africa with the Regional Biomass Model RBM plus, using optimized 250 m MODIS FPAR and fractional vegetation cover information. Int. J. Appl. Earth Obs. Geoinf. 43, 177–194.
Mahadevan, P., Wofsy, S.C., Matross, D.M., Xiao, X.M., Dunn, A.L., Lin, J.C., Gerbig, C., Munger, J.W., Chow, V.Y., Gottlieb, E.W., 2008. A satellite-based biosphere parameterization for net ecosystem CO_2 exchange: Vegetation Photosynthesis and Respiration Model (VPRM). Glob. Biogeochem. Cycles 22, 1–17.
Mandal, B., Majumder, B., Bandyopadhyay, P.K., Hazra, G.C., Gangopadhyay, A., Samantaray, R.N., Mishra, A.K., Chaudhury, J., Saha, M.N., Kundu, S., 2007. The potential of cropping systems and soil amendments for carbon sequestration in soils under long-term experiments in subtropical India. Glob. Chang. Biol. 13, 357–369.
Matthes, J.H., Knox, S.H., Sturtevant, C., Sonnentag, O., Verfaillie, J., Baldocchi, D., 2015. Predicting landscape-scale CO_2 flux at a pasture and rice paddy with long-term hyperspectral canopy reflectance measurements. Biogeosciences 12, 4577–4594.
Min, S.H., Shim, K.M., Kim, Y.S., Jung, M.P., Kim, S.C., So, K.H., 2013. Seasonal variation of carbon dioxide and energy fluxes during the rice cropping season at rice-barley double cropping paddy field of Gimje. Korean J. Agric. For. Meteorol. 15, 273–281.
Min, S.H., Shim, K.M., Kim, Y.S., Hwang, H., Jung, M.P., Choi, I.T., 2014. Seasonal variation of CO_2 exchange during the barley growing season at a rice-barley double cropping paddy field in Gimje, Korea. Korean J. Agric. For. Meteorol. 16, 137–145.
Mizoguchi, Y., Miyata, A., Ohtani, Y., Hirata, R., Yuta, S., 2009. A review of tower flux observation sites in Asia. J. For. Res. 14, 1–9.
Motohka, T., Nasahara, K.N., Miyata, A., Mano, M., Tsuchida, S., 2009. Evaluation of optical satellite remote sensing for rice paddy phenology in monsoon Asia using a continuous in situ dataset. Int. J. Remote Sens. 30, 4343–4357.
Nichol, C.J., Huemmrich, K.F., Black, T.A., Jarvis, P.G., Walthall, C.L., Grace, J., Hall, F.G., 2000. Remote sensing of photosynthetic-light-use efficiency of boreal forest. Agric. For. Meteorol. 101, 131–142.
Ono, K., Mano, M., Han, G.H., Nagai, H., Yamada, T., Kobayashi, Y., Miyata, A., Inoue, Y., Lal, R., 2015. Environmental controls on fallow carbon dioxide flux in a single-crop rice paddy, Japan. Land Degrad. Dev. 26, 331–339.
Pan, G.X., Li, L.Q., Wu, L.S., Zhang, X.H., 2004. Storage and sequestration potential of topsoil organic carbon in China's paddy soils. Glob. Chang. Biol. 10, 79–92.
Potter, C.S., 1999. Terrestrial biomass and the effects of deforestation on the global carbon cycle—results from a model of primary production using satellite observations. Bioscience 49, 769–778.
Potter, C.S., Randerson, J.T., Field, C.B., Matson, P.A., Vitousek, P.M., Mooney, H.A., Klooster, S.A., 1993. Terrestrial ecosystem production—a process model-based on global satellite and surface data. Glob. Biogeochem. Cycles 7, 811–841.
Prather, M., Ehhalt, D., 2001. Atmospheric chemistry and greenhouse gases. In: Houghton, J.T., Ding, Y., Griggs, D.J., Noguer, M., van der Linden, P.J., Dai, X., Maskell, K., Johnson, C.A. (Eds.), Climate Change 2001: The Scientific Basis. Cambridge University Press, Cambridge, U.K., pp. 239–287.
Prince, S.D.a.S.J.G., 1995. Global primary production: a remote sensing approach. J. Biogeogr. 22, 316–336.
Propastin, P., Ibrom, A., Knohl, A., Erasmi, S., 2012. Effects of canopy photosynthesis saturation on the estimation of gross primary productivity from MODIS data in a tropical forest. Remote Sens. Environ. 121, 252–260.
Raich, J.W., Rastetter, E.B., Melillo, J.M., Kicklighter, D.W., Steudler, P.A., Peterson, B.J., Grace, A.L., Moore, B., Vorosmarty, C.J., 1991. Potential net primary productivity in South-America-application of a global-model. Ecol. Appl. 1, 399–429.
Reichstein, M., Falge, E., Baldocchi, D., Papale, D., Aubinet, M., Berbigier, P., Bernhofer, C., Buchmann, N., Gilmanov, T., Granier, A., Grunwald, T., Havrankova, K., Ilvesniemi, H., Janous, D., Knohl, A., Laurila, T., Lohila, A., Loustau, D., Matteucci, G., Meyers, T., Miglietta, F., Ourcival, J.-M., Pumpanen, J., Rambal, S., Rotenberg, E., Sanz, M., Tenhunen, J., Seufert, G., Vaccari, F., Vesala, T., Yakir, D., Valentini, R., 2005. On the separation of net ecosystem exchange into assimilation and ecosystem respiration: review and improved algorithm. Glob. Chang. Biol. 11, 1424–1439.
Ren, X.E., Wang, Q.X., Tong, C.L., Wu, J.S., Wang, K.L., Zhu, Y.L., Lin, Z.J., Masataka, W., Tang, G.Y., 2007. Estimation of soil respiration in a paddy ecosystem in the subtropical region of China. Chin. Sci. Bull. 52, 2722–2730.
Ren, X.L., He, H.L., Zhang, L., Zhou, L., Yu, G.R., Fan, J.W., 2013. Spatiotemporal variability analysis of diffuse radiation in China during 1981–2010. Ann. Geophys. 31, 277–289.
Rossini, M., Meroni, M., Migliavacca, M., Manca, G., Cogliati, S., Busetto, L., Picchi, V., Cescatti, A., Seufert, G., Colombo, R., 2010. High resolution field spectroscopy measurements for estimating gross ecosystem production in a rice field. Agric. For. Meteorol. 150, 1283–1296.
Running, S.W., Baldocchi, D.D., Turner, D.P., Gower, S.T., Bakwin, P.S., Hibbard, K.A., 1999. A global terrestrial monitoring network integrating tower fluxes, flask sampling, ecosystem modeling and EOS satellite data. Remote Sens. Environ. 70, 108–127.

Running, S.W., Thornton, P.E., Nemani, R., Glassy, J.M., 2000. Global terrestrial gross and net primary productivity from the Earth Observing System. In: Sala, O.E., Jackson, R.B., Mooney, H.A., Howarth, R.W. (Eds.), Methods in Ecosystem Science. Springer Verlag, New York, pp. 44–57.

Running, S.W., Nemani, R.R., Heinsch, F.A., Zhao, M.S., Reeves, M., Hashimoto, H., 2004. A continuous satellite-derived measure of global terrestrial primary production. Bioscience 54, 547–560.

Ryu, Y., Kang, S., Moon, S.-K., Kim, J., 2008. Evaluation of land surface radiation balance derived from moderate resolution imaging spectroradiometer (MODIS) over complex terrain and heterogeneous landscape on clear sky days. Agric. For. Meteorol. 148, 1538–1552.

Saito, M., Miyata, A., Nagai, H., Yamada, T., 2005. Seasonal variation of carbon dioxide exchange in rice paddy field in Japan. Agric. For. Meteorol. 135, 93–109.

Salvucci, M.E., Osteryoung, K.W., Crafts-Brandner, S.J., Vierling, E., 2001. Exceptional sensitivity of Rubisco activase to thermal denaturation in vitro and in vivo. Plant Physiol. 127, 1053–1064.

Sanchez, M.L., Pardo, N., Perez, I.A., Garcia, M.A., 2015. GPP and maximum light use efficiency estimates using different approaches over a rotating biodiesel crop. Agric. For. Meteorol. 214, 444–455.

Seaquist, J.W., Olsson, L., Ardo, J., 2003. A remote sensing-based primary production model for grassland biomes. Ecol. Model. 169, 131–155.

Shim, K.M., Min, S.H., Kim, Y.S., Jung, M.P., Choi, I.T., 2015. Estimation of net biome production in a barley-rice double cropping paddy field of Gimje, Korea. Korean J. Agric. For. Meteorol. 17, 173–181.

Sims, D.A., Rahman, A.F., Cordova, V.D., El-Masri, B.Z., Baldocchi, D.D., Flanagan, L.B., Goldstein, A.H., Hollinger, D.Y., Misson, L., Monson, R.K., Oechel, W.C., Schmid, H.P., Wofsy, S.C., Xu, L.K., 2006. On the use of MODIS EVI to assess gross primary productivity of North American ecosystems. J. Geophys. Res. Biogeosci. 111, 1–16.

Sims, D., Rahman, A., Cordova, V., Elmasri, B., Baldocchi, D., Bolstad, P., Flanagan, L., Goldstein, A., Hollinger, D., Misson, L., 2008. A new model of gross primary productivity for North American ecosystems based solely on the enhanced vegetation index and land surface temperature from MODIS. Remote Sens. Environ. 112, 1633–1646.

Singh, R.P., Oza, S.R., Pandya, M.R., 2006. Observing long-term changes in rice phenology using NOAA-AVHRR and DMSP-SSM/I satellite sensor measurements in Punjab, India. Curr. Sci. 91, 1217–1221.

Sjöström, M., Zhao, M., Archibald, S., Arneth, A., Cappelaere, B., Falk, U., de Grandcourt, A., Hanan, N., Kergoat, L., Kutsch, W., Merbold, L., Mougin, E., Nickless, A., Nouvellon, Y., Scholes, R.J., Veenendaal, E.M., Ardö, J., 2013. Evaluation of MODIS gross primary productivity for Africa using eddy covariance data. Remote Sens. Environ. 131, 275–286.

Stockli, R., Lawrence, D.M., Niu, G.Y., Oleson, K.W., Thornton, P.E., Yang, Z.L., Bonan, G.B., Denning, A.S., Running, S.W., 2008. Use of FLUXNET in the community land model development. J. Geophys. Res. Biogeosci. 113, 1–19.

Tang, X.G., Li, H.P., Huang, N., Li, X.Y., Xu, X.B., Ding, Z., Xie, J., 2015a. A comprehensive assessment of MODIS-derived GPP for forest ecosystems using the site-level FLUXNET database. Environ. Earth Sci. 74, 5907–5918.

Tang, X.G., Li, H.P., Liu, G.H., Li, X.Y., Yao, L., Xie, J., Chang, S.Z., 2015b. Sensitivity of near real-time MODIS gross primary productivity in terrestrial forest based on eddy covariance measurements. Chin. Geogr. Sci. 25, 537–548.

Tokida, T., Fumoto, T., Cheng, W., Matsunami, T., Adachi, M., Katayanagi, N., Matsushima, M., Okawara, Y., Nakamura, H., Okada, M., Sameshima, R., Hasegawa, T., 2010. Effects of free-air CO_2 enrichment (FACE) and soil warming on CH_4 emission from a rice paddy field: Impact assessment and stoichiometric evaluation. Biogeosciences 7, 2639–2653.

Tucker, C.J., 1979. Red and photographic infrared linear combinations for monitoring vegetation. Remote Sens. Environ. 8, 127–150.

Wagle, P., Xiao, X., Torn, M.S., Cook, D.R., Matamala, R., Fischer, M.L., Jin, C., Dong, J., Biradar, C., 2014. Sensitivity of vegetation indices and gross primary production of tallgrass prairie to severe drought. Remote Sens. Environ. 152, 1–14.

Wagle, P., Xiao, X., Suyker, A.E., 2015. Estimation and analysis of gross primary production of soybean under various management practices and drought conditions. ISPRS J. Photogramm. Remote Sens. 99, 70–83.

Wang, H., Li, X.B., Long, H.L., Zhu, W.Q., 2009. A study of the seasonal dynamics of grassland growth rates in Inner Mongolia based on AVHRR data and a light-use efficiency model. Int. J. Remote Sens. 30, 3799–3815.

Wang, Z., Xiao, X., Yan, X., 2010. Modeling gross primary production of maize cropland and degraded grassland in northeastern China. Agric. For. Meteorol. 150, 1160–1167.

Williams, M., Richardson, A.D., Reichstein, M., Stoy, P.C., Peylin, P., Verbeeck, H., Carvalhais, N., Jung, M., Hollinger, D.Y., Kattge, J., Leuning, R., Luo, Y., Tomelleri, E., Trudinger, C.M., Wang, Y.P., 2009. Improving land surface models with FLUXNET data. Biogeosciences 6, 1341–1359.

Wu, W.X., Wang, S.Q., Xiao, X.M., Yu, G.R., Fu, Y.L., Hao, Y.B., 2008. Modeling gross primary production of a temperate grassland ecosystem in Inner Mongolia, China, using MODIS imagery and climate data. Sci. China Ser. D Earth Sci. 51, 1501–1512.

Wu, C.Y., Niu, Z., Gao, S.A., 2010. Gross primary production estimation from MODIS data with vegetation index and photosynthetically active radiation in maize. J. Geophys. Res.-Atmos. 115.

Wu, C.Y., Chen, J.M., Desai, A.R., Hollinger, D.Y., Arain, M.A., Margolis, H.A., Gough, C.M., Staebler, R.M., 2012. Remote sensing of canopy light use efficiency in temperate and boreal forests of North America using MODIS imagery. Remote Sens. Environ. 118, 60–72.

Xia, J.Y., Niu, S.L., Ciais, P., Janssens, I.A., Chen, J.Q., Ammann, C., Arain, A., Blanken, P.D., Cescatti, A., Bonal, D., Buchmann, N., Curtis, P.S., Chen, S.P., Dong, J.W., Flanagan, L.B., Frankenberg, C., Georgiadis, T., Gough, C.M., Hui, D.F., Kiely, G., Li, J.W., Lund, M., Magliulo, V., Marcolla, B., Merbold, L., Montagnani, L., Moors, E.J., Olesen, J.E., Piao, S.L., Raschi, A., Roupsard, O., Suyker, A.E., Urbaniak, M., Vaccari, F.P., Varlagin, A., Vesala, T., Wilkinson, M., Weng, E., Wohlfahrt, G., Yan, L.M., Luo, Y.Q., 2015. Joint control of terrestrial gross primary productivity by plant phenology and physiology. Proc. Natl. Acad. Sci. U. S. A. 112, 2788–2793.

Xiao, X., Boles, S., Frolking, S., Salas, W., Moore, B., Li, C., He, L., Zhao, R., 2002. Observation of flooding and rice transplanting of paddy rice fields at the site to landscape scales in China using VEGETATION sensor data. Int. J. Remote Sens. 23, 3009–3022.

Xiao, X.M., Hollinger, D., Aber, J., Goltz, M., Davidson, E.A., Zhang, Q.Y., Moore, B., 2004a. Satellite-based modeling of gross primary production in an evergreen needleleaf forest. Remote Sens. Environ. 89, 519–534.

Xiao, X.M., Zhang, Q.Y., Braswell, B., Urbanski, S., Boles, S., Wofsy, S., Berrien, M., Ojima, D., 2004b. Modeling gross primary production of temperate deciduous broadleaf forest using satellite images and climate data. Remote Sens. Environ. 91, 256–270.

Xiao, X.M., Zhang, Q.Y., Hollinger, D., Aber, J., Moore, B., 2005a. Modeling gross primary production of an evergreen needleleaf forest using modis and climate data. Ecol. Appl. 15, 954–969.

Xiao, X.M., Zhang, Q.Y., Saleska, S., Hutyra, L., De Camargo, P., Wofsy, S., Frolking, S., Boles, S., Keller, M., Moore, B., 2005b. Satellite-based modeling of gross primary production in a seasonally moist tropical evergreen forest. Remote Sens. Environ. 94, 105–122.

Xiao, X., Zhang, J., Yan, H., Wu, W., Biradar, C., 2009. Land surface phenology. In: Noormets, A. (Ed.), Phenology of Ecosystem Processes: Applications in Global Change Research. Springer New York, New York, NY, pp. 247–270.

Xiao, J.F., Davis, K.J., Urban, N.M., Keller, K., Saliendra, N.Z., 2011. Upscaling carbon fluxes from towers to the regional scale: influence of parameter variability and land cover representation on regional flux estimates. J. Geophys. Res. Biogeosci. 116, 15.

Yamori, W., Hikosaka, K., Way, D.A., 2014. Temperature response of photosynthesis in C_3, C_4, and CAM plants: temperature acclimation and temperature adaptation. Photosynth. Res. 119, 101–117.

Yan, H.M., Fu, Y.L., Xiao, X.M., Huang, H.Q., He, H.L., Ediger, L., 2009. Modeling gross primary productivity for winter wheat-maize double cropping system using MODIS time series and CO_2 eddy flux tower data. Agric. Ecosyst. Environ. 129, 391–400.

Yang, S.H., Xu, J.Z., Liu, X.Y., Zhang, J.G., Wang, Y.J., 2016. Variations of carbon dioxide exchange in paddy field ecosystem under water-saving irrigation in Southeast China. Agric. Water Manag. 166, 42–52.

Yuan, W.P., Liu, S., Zhou, G.S., Zhou, G.Y., Tieszen, L.L., Baldocchi, D., Bernhofer, C., Gholz, H., Goldstein, A.H., Goulden, M.L., Hollinger, D.Y., Hu, Y., Law, B.E., Stoy, P.C., Vesala, T., Wofsy, S.C., AmeriFlux, C., 2007. Deriving a light use efficiency model from eddy covariance flux data for predicting daily gross primary production across biomes. Agric. For. Meteorol. 143, 189–207.

Yuan, W., Cai, W., Nguy-Robertson, A.L., Fang, H., Suyker, A.E., Chen, Y., Dong, W., Liu, S., Zhang, H., 2015. Uncertainty in simulating gross primary production of cropland ecosystem from satellite-based models. Agric. For. Meteorol. 207, 48–57.

Zhang, Q.Y., Xiao, X.M., Braswell, B., Linder, E., Ollinger, S., Smith, M.L., Jenkins, J.P., Baret, F., Richardson, A.D., Moore, B., Minocha, R., 2006. Characterization of seasonal variation of forest canopy in a temperate deciduous broadleaf forest, using daily MODIS data. Remote Sens. Environ. 105, 189–203.

Zhang, Q.Y., Middleton, E.M., Margolis, H.A., Drolet, G.G., Barr, A.A., Black, T.A., 2009. Can a satellite-derived estimate of the fraction of PAR absorbed by chlorophyll ($FAPAR_{chl}$) improve predictions of light-use efficiency and ecosystem photosynthesis for a boreal aspen forest? Remote Sens. Environ. 113, 880–888.

Zhang, Q.Y., Middleton, E.M., Cheng, Y.B., Landis, D.R., 2013. Variations of foliage chlorophyll fAPAR and foliage non-chlorophyll fAPAR ($fAPAR_{chl}$, $fAPAR_{non\text{-}chl}$) at the Harvard Forest. IEEE J. Sel. Top. Appl. Earth Obs. Remote Sens. 6, 2254–2264.

Zhang, X.X., Fan, C.H., Ma, Y.C., Liu, Y.L., Li, L., Zhou, Q.S., Xiong, Z.Q., 2014. Two approaches for net ecosystem carbon budgets and soil carbon sequestration in a rice-wheat rotation system in China. Nutr. Cycl. Agroecosyst. 100, 301–313.

Zhang, Y., Xiao, X., Jin, C., Dong, J., Zhou, S., Wagle, P., Joiner, J., Guanter, L., Zhang, Y., Zhang, G., Qin, Y., Wang, J., Moore, B., 2016. Consistency between sun-induced chlorophyll fluorescence and gross primary production of vegetation in North America. Remote Sens. Environ. 183, 154–169.

Zhao, M.S., Running, S.W., 2010. Drought-induced reduction in global terrestrial net primary production from 2000 through 2009. Science 329, 940–943.

Zhao, M.S., Heinsch, F.A., Nemani, R.R., Running, S.W., 2005. Improvements of the MODIS terrestrial gross and net primary production global data set. Remote Sens. Environ. 95, 164–176.

Zhao, M., Running, S.W., Nemani, R.R., 2006. Sensitivity of Moderate Resolution Imaging Spectroradiometer (MODIS) terrestrial primary production to the accuracy of meteorological reanalyses. J. Geophys. Res. Biogeosci. 111.